NASA CONTRACTOR REPORT

CR-61107

CR-61107

FACILITY FORM 602

| | |
|---|---|
| N66-10690 | |
| (ACCESSION NUMBER) | (THRU) |
| 49 | 1 |
| (PAGES) | (CODE) |
| | 31 |
| (NASA CR OR TMX OR AD NUMBER) | (CATEGORY) |

# THE SCHEDULE OF MEASUREMENTS FOR ANALYSIS OF AN ONBOARD NAVIGATION SYSTEM


Prepared under Contract No. NAS 8-11198 by
Paul J. Rohde

Philco Corporation
A Subsidiary of Ford Motor Company
Palo Alto, California


GPO PRICE $ ______

CFSTI PRICE(S) $ ______

Hard copy (HC) 2.00

Microfiche (MF) .50

ff 653 July 65

For

NASA-GEORGE C. MARSHALL SPACE FLIGHT CENTER
Huntsville, Alabama

October 1965

CONTRACTOR REPORT

# THE SCHEDULING OF MEASUREMENTS FOR ANALYSIS OF AN ONBOARD NAVIGATION SYSTEM

Prepared by

PHILCO CORPORATION
WDL Division
Palo Alto, California

## ABSTRACT

10690

This document is concerned with the selection of a measurement schedule for an onboard navigation system. The instrument which is considered to be of interest is the sextant or theodolite. Three sets of auxiliary schedule data are presented to act as engineering guides in the selection of stars and planetary bodies along the trajectory of interest. The use of this auxiliary data is demonstrated along a round trip Mars trajectory and a lunar trajectory. The value of using the auxiliary data as a guide is verified by obtaining tracking schedule evaluation data from a digital computer simulation of an onboard tracking system.

Author

October 15, 1965 CR-61107

# THE SCHEDULE OF MEASUREMENTS FOR ANALYSIS OF AN ONBOARD NAVIGATION SYSTEM

By

Paul J. Rohde

Prepared under Contract No. NAS 8-11198 by

PHILCO CORPORATION
A Subsidiary of Ford Motor Company
Palo Alto, California

For

Astrionics Laboratory

NASA- GEORGE C. MARSHALL SPACE FLIGHT CENTER

TABLE OF CONTENTS

## LIST OF ILLUSTRATIONS

CONTRACTOR REPORT

# THE SCHEDULING OF MEASUREMENTS FOR ANALYSIS OF AN ONBOARD NAVIGATION SYSTEM


## SUMMARY

This document is concerned with the selection of a measurement schedule for an onboard navigation system. The instruments which are considered to be of interest are the sextant and the theodolite. Three sets of auxiliary schedule data are presented to act as engineering guides in the selection of stars and planetary bodies along the trajectory of interest. The use of this auxiliary data is demonstrated along a round-trip Mars trajectory and a lunar trajectory. The value of using the auxiliary data as a guide is verified by obtaining tracking schedule evaluation data from a digital computer simulation of an onboard tracking system.

# SECTION I. INTRODUCTION

One of the problems associated with studies of navigation instrumentation requirements of space missions is the selection of a measurement schedule for the onboard instrumentation. This problem usually arises for manned missions where it is desirable to provide the capability of navigation, but it can arise in unmanned probes when a high-accuracy orbit relative to the target body is needed to fulfill the mission objectives.

The basic difficulty is that it is not feasible to calculate data for all of the large number of possible schedules and observations. One usually is interested in establishing which observations are the most important on a given schedule and the effect of scheduling. To plan data runs to establish the interrelationships between these factors, some guidelines are needed. In addition, since each datum calculation on a digital computer requires a reasonable amount of time, it is desirable to organize the calculations such that every run provides as much information as possible.

Some of the basic problems associated with onboard navigation are discussed in this document, and suggestions are made as to certain auxiliary data which can be calculated prior to the navigation study. It is believed that this auxiliary data is quite useful in forming the engineering type of guidelines needed to reduce the number of observation schedules to be evaluated.

These data are certain quantities calculated on the nominal trajectory* which suggest those measurements which are the most promising as a function of time. The method suggested here is primarily for consideration of a line-of-sight (LOS) type of measurement. This implies the use of a theodolite or sextant type of device where the following questions are important:

1. Which planetary body should be used?
2. Is the Sun in an unfavorable position?
3. What type of requirements are placed on the control system by an observation sequence?

In addition to the above considerations, the use of the sextant requires answers to two more questions.

4. Which stars should be used?
5. Is the star-planetary body angle within specified limits?

The auxiliary data which are presented here have been designed to provide information relevant to answering these questions. Data which are useful aids in answering the first three questions are presented in Section III; the last two questions, which are primarily concerned with the sextant measurement, are answered in Section IV.

---

* The nominal trajectories used in this document are described in Appendix A.

## SECTION II. NAVIGATION MEASUREMENTS

The navigation measurements which are of interest in this document are the two angle measurements required to determine the direction of the line-of-sight (LOS) to a planetary body. These measurements are: (1) right ascension (RA) and declination (DEC) of the body measured in an inertial reference frame when using a theodolite, or (2) two separate star planet angles when using a sextant.

It is assumed that estimates of the spacecraft's position and velocity are known so that perturbation techniques and linear filtering can be employed in using the observation data. As is shown in Appendix B, each angular measurement establishes a component of spacecraft position along some direction in space. The particular direction in which the position is established is described by the gradient of the measurement with respect to the spacecraft's position. This row vector, $\vec{h}$, characterizes each of the measurements which are made. As shown in Appendix B, measurement of the LOS direction establishes the spacecraft's position in a plane normal to the LOS direction. The measurement deviation from the nominal value may be written as:

$$\delta q = \vec{h} \cdot x \tag{1}$$

where:

$\delta q$ = deviation of measurement value from nominal value

$\vec{h}$ = gradient of measurement with respect to vehicle's position state

$x$ = position state deviation from nominal.

In order to be able to establish the spacecraft's total position state deviation from the nominal at a given time, a minimum of three measurements must be made. The set of measurements would be described by the three associated $\vec{h}$ vectors as shown below.

$$\begin{pmatrix} \delta q_1 \\ \delta q_2 \\ \delta q_3 \end{pmatrix} = \begin{pmatrix} \vec{h}_1 \\ \vec{h}_2 \\ \vec{h}_3 \end{pmatrix} \cdot x \tag{2}$$

where 1, 2, and 3 refer to the three measurements.

Defining the residuals, $\delta q_1$, $\delta q_2$, $\delta q_3$ as a vector, Q, and the three $\vec{h}$ vectors as a 3 x 3 matrix H, Equation 2 may be written as:

$$Q = H\,x \tag{3}$$

This equation may be solved for the position deviation state, x, in the following manner if H is invertible.

$$x = H^{-1}Q \tag{4}$$

The existence of $H^{-1}$ requires that none of the $\vec{h}$ vectors is zero nor is one vector linearly dependent on the other two vectors. Then the total position deviation state may be obtained as shown by Equation (4).

A consideration of the errors associated with the measurements indicates the desirability of having the $\vec{h}$ vectors not only linearly independent but also near orthogonal. If a two-dimensional problem is considered with two measurements being made, the measurement errors may be pictorially represented as shown in Figure 1. In Figure 1, one observation is made of each body, A and B.

In both cases shown, the measurement vectors $\vec{h}_A$ and $\vec{h}_B$ are independent so that the position in the plane could be established. The difference between the two cases is illustrated by the cross-hatched sections in the figure. These pictorially represent the standard deviation of the position estimate obtained with the measurements of the direction of the LOS to planets A and B. The desirability of having the $\vec{h}$ vectors in orthogonal directions is apparent.

These basic measurement properties which have been presented here will be used in the analysis of the auxiliary data to be presented in Sections III and IV.

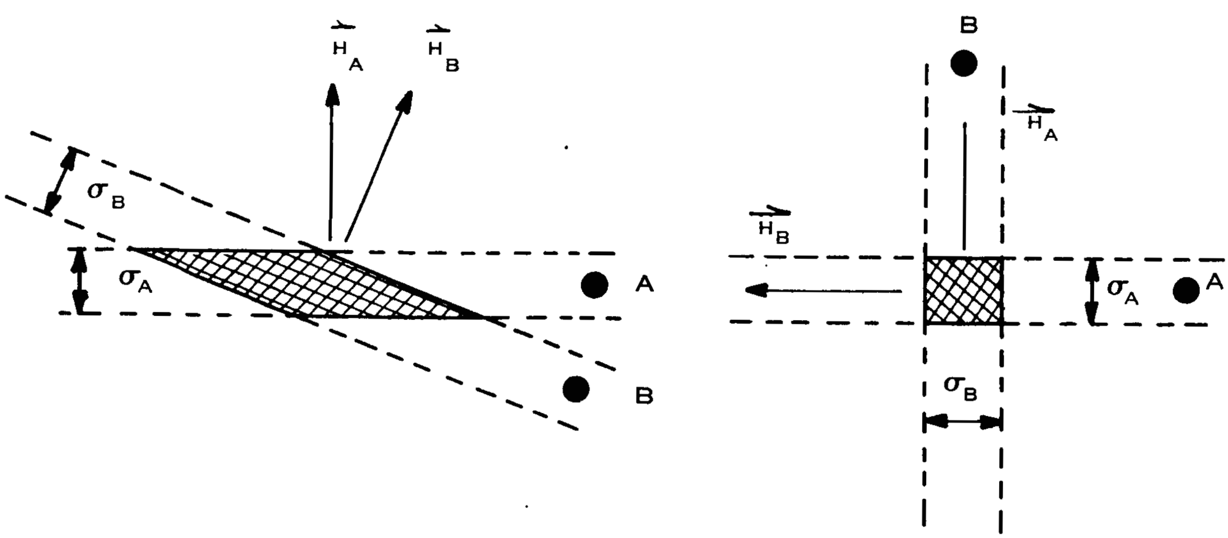


FIGURE 1. MEASUREMENT ERRORS FOR A TWO-DIMENSIONAL PROBLEM

## SECTION III. PLANETARY BODY SELECTION

### A. GENERAL

In this section, auxiliary data will be presented to act as a guide in the selection of those planetary bodies which are to be used for navigation measurements. In the case of selection of a body for use with a sextant, the selection of the bodies will have to also be evaluated for presence of stars as shown in Section IV.

The discussion of the onboard navigation measurement in Section II indicated the following three important factors are to be considered when making measurements:

1. Accuracy of measurement being performed.
2. Direction of the $\vec{h}$ vector which characterizes a measurement.
3. Relative directions of the $\vec{h}$ vectors associated with a set of observations.

These three factors were used as guides in selecting the type of auxiliary data which would provide valuable information for the selection of planetary bodies.

### B. MEASUREMENT ACCURACY

Quite obviously the measurement accuracy which is attainable with a given instrument is one of the fundamental characteristics which describes an onboard navigation system. For optical devices, this accuracy is usually specified in terms of minutes or seconds of arc. Since the measurement error is an angular error, the position uncertainty established with such a device is directly related to the range of the body being observed. Thus, the uncertainty in a position measurement, $\epsilon_p$, for a single observation of a body is

$$\epsilon_p = \sigma_\epsilon \left|R\right| \tag{5}$$

$\left|R\right|$ = Range to planet

$\sigma_\epsilon$ = Measurement error (standard deviation)

One can therefore use Equation (5) to calculate the uncertainty in a position measurement when using each of the celestial bodies of interest along a nominal trajectory. The angular measurement error, $\sigma_\epsilon$, for the instrument must be specified.

The standard deviation of the angular measurement error was assumed to be:

$$\sigma_\epsilon = \sqrt{k_1^2 + 4k_2^2 \left(\sin^{-1} \frac{RAD}{|R|}\right)^2} \tag{6}$$

where

$k_1^2$ = the variance of the angular error when the instrument is used for star-star measurements

$k_2^2$ = the variance of the angular error when the instrument is used to measure the subtended angle of the body at some low altitude

RAD = radius of the body

$|R|$ = range to body center

The error model given by Equation (6) is based on the assumption that as the body is approached, its size in the field of view increases, thus causing a greater error in detecting the apparent center (or RIM). It is likely that the magnitude of the total LOS rate should also enter in this error model due to the difficulties of tracking a moving object. This LOS rate effect was neglected due to lack of information on how to include this effect.

Figure 2A shows the error in position estimate for a single observation as calculated using Equations (5) and (6) along the Earth-Mars nominal trajectory. The figure shows the quantity $\epsilon_p$ as a function of time for several celestial bodies of interest. As can be seen, the Earth and Moon provide the smallest position uncertainty, early in the flight. In the middle of the flight, the Earth, Moon, Sun, Venus, and Mars are about the same (approximately 10,000 km uncertainty). At the end of the flight, Mars has by far the smallest position uncertainty. This data shows that Jupiter is not of importance in selecting a schedule, because the position measurement error for this body is very large for all of the flight.

It is of interest to note that in evaluating the ordinate of Figure 2A (in the case of random uncorrelated errors), the variance in the estimate of a parameter, $\sigma_{EST}$, reduces as the square root of the number of observations, N,:

$$\sigma_{EST} = \frac{\sigma_{MEAS}}{\sqrt{N}} \tag{7}$$

Therefore, an order of magnitude difference in the accuracy of a position estimate obtained using one body as opposed to another implies that 100 of the poorer measurements must be made for each good measurement in order to obtain an equally accurate estimate. This example illustrates the extreme importance of the data shown in Figure 2A as a guide in selecting the body or bodies to be used as a function of time.

## C. DIRECTION OF LINE-OF-SIGHT

The direction of the LOS to a planetary body as observed from a spacecraft is important in establishing the value of using that body on a navigation schedule. As indicated in Section III, B, the accuracy of a measurement is an

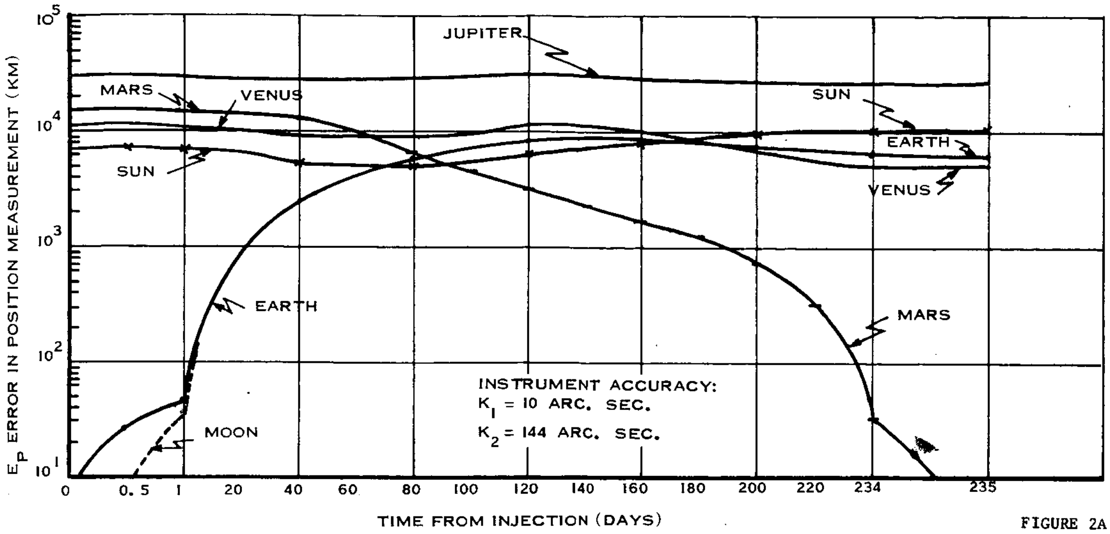


FIGURE 2A

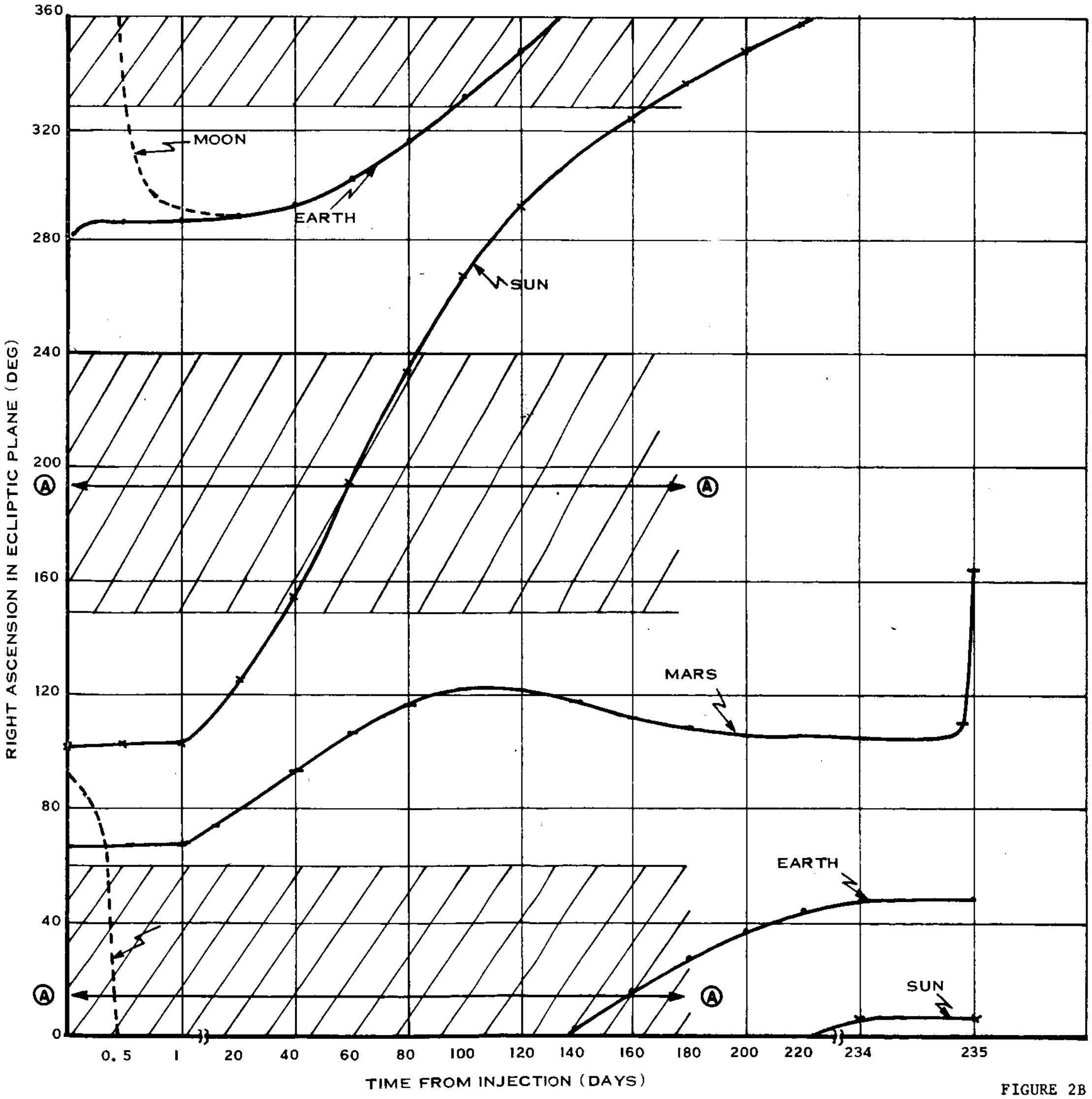


FIGURE 2B

FIGURE 2. SCHEDULE DATA FOR EARTH-MARS TRAJECTORY

important consideration in selecting a body, but the orientation of the measurement vector, $\vec{h}$, is equally important. The reason for the importance of the LOS direction is that there is a particular relationship between the direction of the LOS to a body and the $\vec{h}$ vectors associated with the measurements used to determine the direction of the LOS. This relationship is shown in Appendix B and illustrated in Figure 3. The two $\vec{h}$ vectors associated with the LOS direction measurement span a plane normal to the direction of the LOS. Therefore, the spacecraft's position can be determined in a plane normal to the LOS direction. Position along the LOS direction is not determined by the measurements. The selection of a second body for observation which had an LOS direction which was nearly orthogonal to the first would then yield the measurement vector required to span the third coordinate of position. This situation would correspond to having a set of $\vec{h}$ vectors which were orthogonal and spanned the total position space.

In order to simplify the presentation of the LOS direction data, it is desirable to resolve the position determination problem into two separate parts. Because the trajectory plane and the orbit planes of all the planetary bodies of interest are nearly parallel to the ecliptic during the midphases of an interplanetary trajectory, the problem can be resolved by: (1) considering the determination of the position normal to the trajectory plane (and ecliptic), and (2) determining the two-dimensional position in the trajectory plane (and ecliptic).

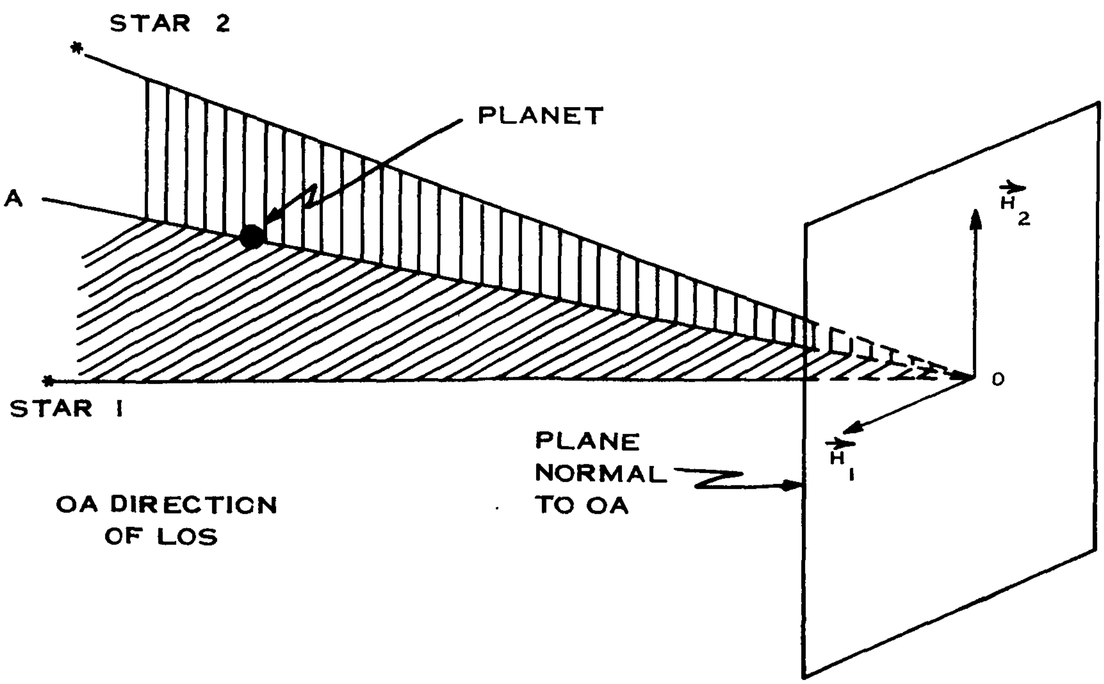


FIGURE 3. RELATIONSHIP BETWEEN THE DIRECTION OF THE LOS TO A BODY AND THE $\vec{h}$ VECTORS ASSOCIATED WITH THE MEASUREMENTS USED TO DETERMINE THE DIRECTION OF THE LOS

Because of the fact that all the planes are nearly parallel to the ecliptic, the $\hat{t}$ measurement direction (normal to the LOS rate as described in Section IV, B) for all the planetary bodies is in the same inertial direction, normal to the ecliptic. Therefore, the position coordinate normal to the trajectory plane may be determined at all times by using any of the bodies with an appropriate star. It is therefore reasonable to use the body which yields the most accurate measurement when determining this coordinate.

The problem of determining the two dimensional position in the trajectory plane is more difficult. In this case, one body at any one time will not provide measurement $\vec{h}$ vectors which span the plane of interest, the trajectory plane. The selection of bodies to be used and the decision as to when they should be used is determined by the in-plane geometry. The selection of the bodies is made on a geometrical basis in conjunction with the other constraint considerations which are discussed in Section IV and the position measurement accuracy. The problem to be solved is shown pictorially in Figure 4. The small arrows represent the $\vec{h}$ vector associated with each planetary body.

The bodies to be observed should be selected such that the associated $\vec{h}$ vectors will span the trajectory plane.

As can be seen from Figure 4, it would be a valuable guide if the RA of the bodies were presented as a function of time in a vehicle-centered, non-rotating coordinate frame. This data would aid in selecting bodies for use when they are ideally positioned relative to the vehicle to determine the vehicle's in-plane position. The RA data have been generated for three bodies, along the Earth-Mars trajectory (see Figure 2B). The selection of these bodies for evaluation was based on the measurement accuracy data shown in Figure 2A.

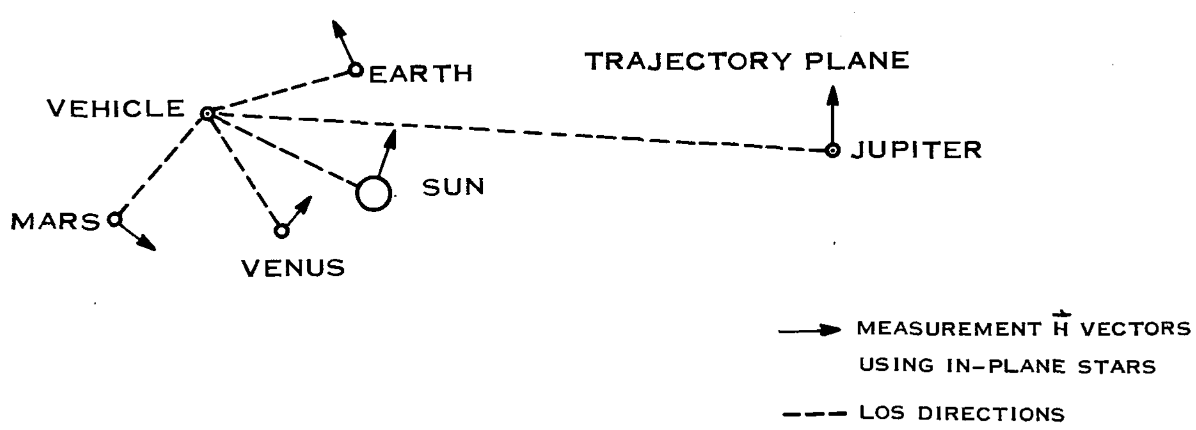


FIGURE 4. PROBLEM OF DETERMINING THE TWO-DIMENSIONAL POSITION IN THE TRAJECTORY PLANE

The usefulness of the data shown in Figure 2 and similar data in Figures 5 and 6 for the Mars-Earth and lunar trajectories in setting up an onboard observation schedule will be demonstrated in Section III, D.

## D. BODY SELECTION EXAMPLES

Onboard tracking schedules have been evaluated to provide quantitative verification of the use of the auxiliary data presented in Section III, B and C. The data have been generated by means of a digital computer error propagation program. This program is a simulation of an onboard navigation system using either a theodolite or sextant for the observation instrument. The program weights all the measurements in an optimum statistical sense (Kalman Filter); thus each new measurement reduces the error in estimate of the miss at encounter.

1. Earth-Mars Trajectory. The auxiliary data for the Earth-Mars trajectory are shown in Figure 2. The star selection data for use with a sextant are shown in Section IV, B. The measurement accuracy data for the individual bodies shown in Figure 2A indicates that the bodies of interest are Earth, Mars, and the Sun. The moon appears as a fine measurement if its use is warranted. Reliance on the use of the moon for navigation data would possibly place an unnecessary constraint on the launch date for an interplanetary trajectory. In the case of the trajectory being used, the moon is in an ideal position to provide good tracking data.

The importance of using the earth early in the flight and Mars late in the flight for navigation data is readily apparent from the good position measurement accuracy (10-100 km) attainable at these times. Also evident is the fact that Jupiter is an unimportant body on this trajectory. The sun appears to be the body which might be of value as a second body during the first half of the flight. The next type of auxiliary data to be used is that shown in Figure 2B. Recalling that the direction of the LOS measurement will determine the position coordinate normal to the LOS direction, the use of the selected bodies can be evaluated for their ability to determine the inplane coordinates.

(The most accurate measurement as a function of time will be used to establish the position coordinate normal to the trajectory plane.)

Neglecting the use of the moon temporarily, the positions of the earth and sun are of interest early in the flight. In the first 30 minutes the direction of the earth's LOS moves from 180 degrees to 280 degrees. The earth's direction then remains relatively constant for approximately 40 days. Neglecting the data which might be obtained during the first 30 minutes using earth observations, the position coordinate which is being determined by the good earth observations is shown by the A - A line segments (normal to the LOS) in Figure 2B. The use of the sun during the early part of the flight does not appear to be of value because of two factors. First, the direction of the sun is very nearly colinear with the direction of the earth (184 degrees away). Therefore, measurements of the direction of the LOS to the sun would again determine the position coordinate along the A - A direction. Second, the measurement accuracy when using the sun is about two orders of magnitude poorer than that obtained using the earth. The effect of using both an earth and a sun observation is shown pictorially in

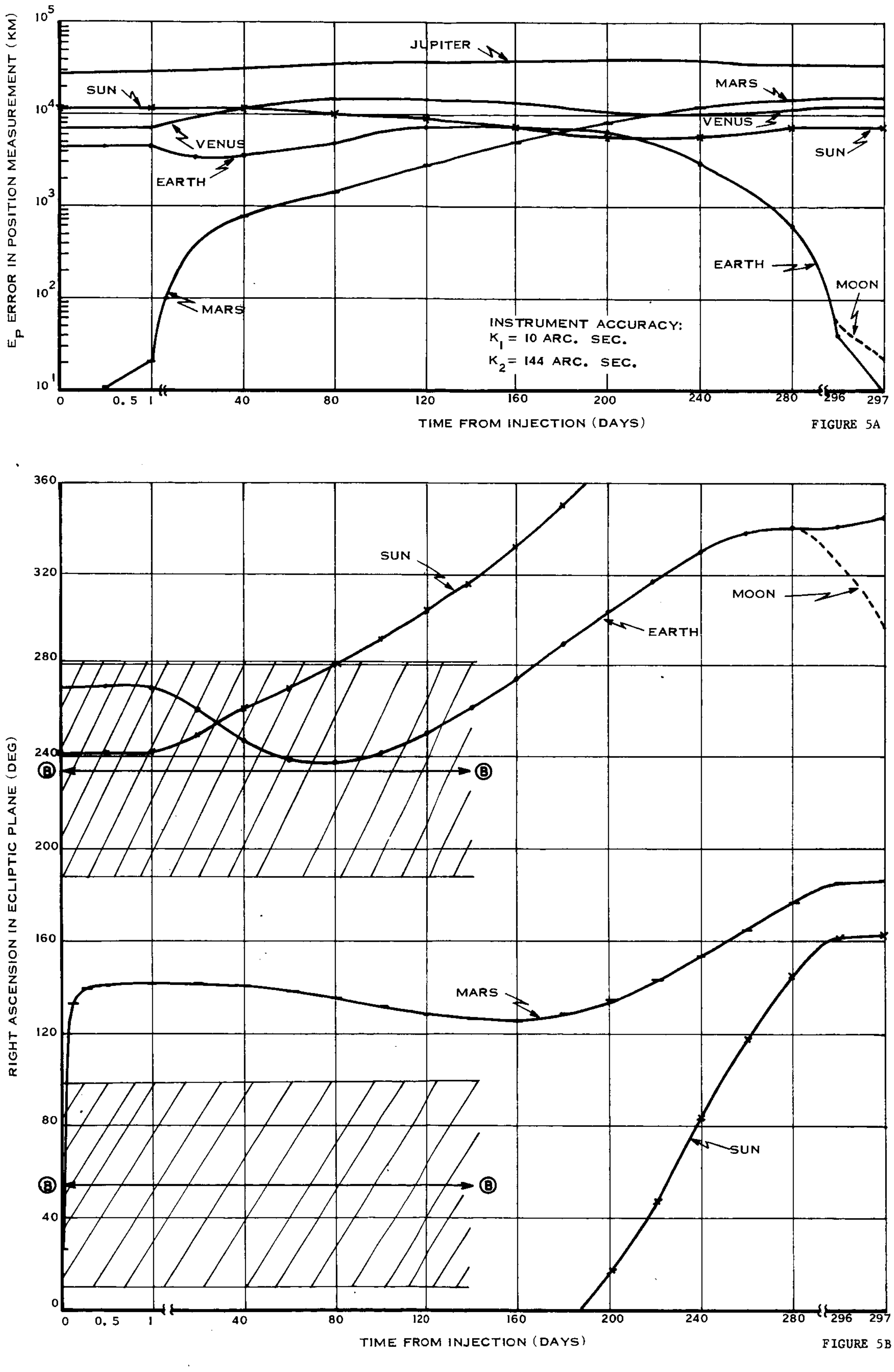


FIGURE 5. SCHEDULE DATA FOR MARS-EARTH TRAJECTORY

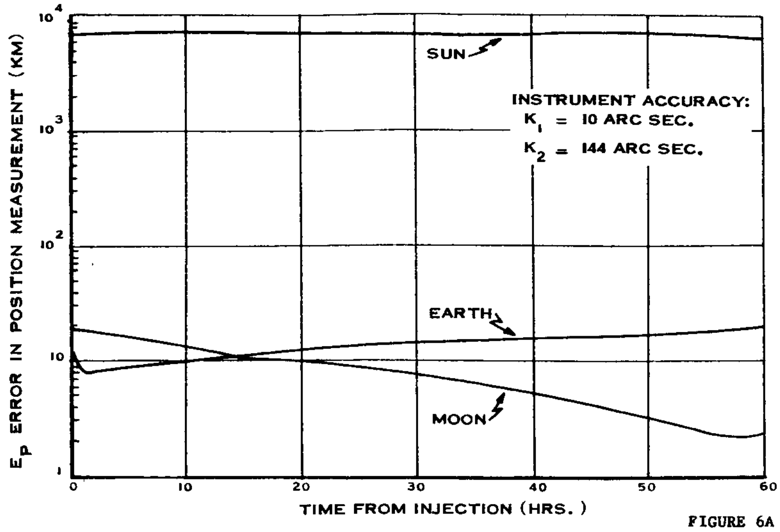


FIGURE 6A

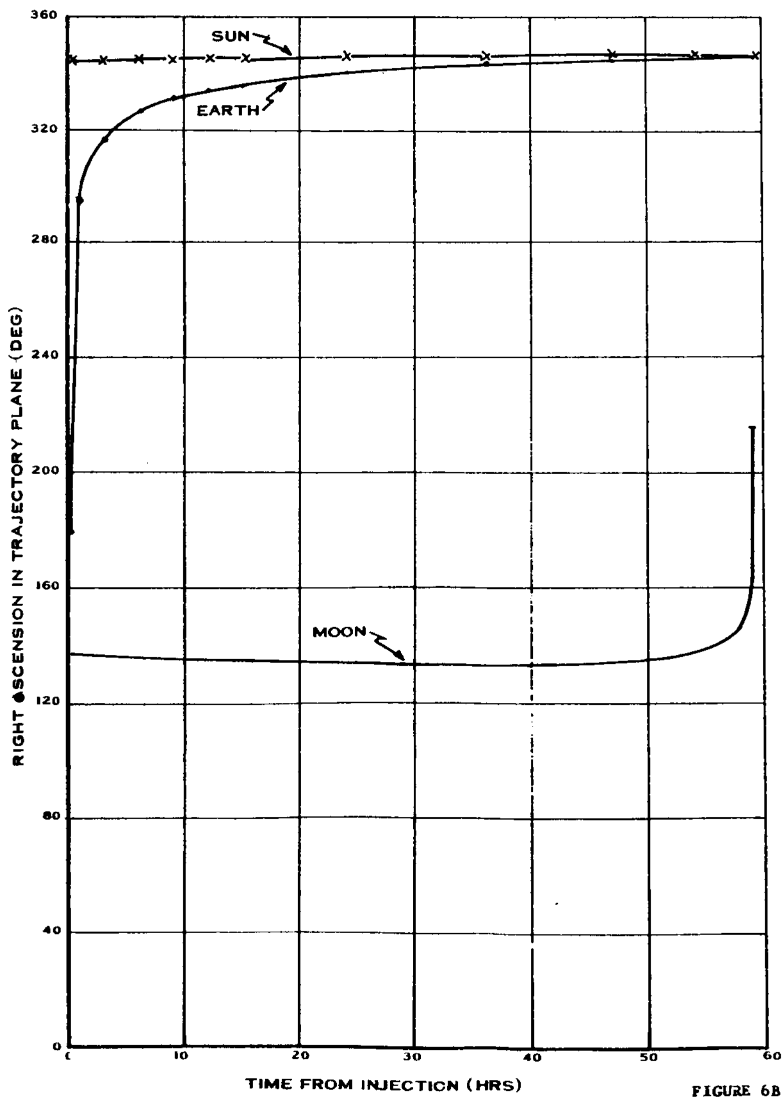


FIGURE 6B

FIGURE 6. SCHEDULE DATA FOR LUNAR TRAJECTORY

Figure 7. The figure illustrates (not to scale) the relative importance of the two measurements by the thick lines along the $\vec{h}$ vectors. It shows that the uncertainty in position along the A - A direction is reduced by the Earth measurement to a point that the Sun measurement with the large error associated with it adds very little information. Neither measurement provides position information along the Earth-Sun line (normal to A - A). These facts are borne out by the tracking data shown in Figure 8. The ordinate is the error in estimate of B•T and B•R at the end point due to errors in the estimate of position and velocity at the time shown. The number one curves were generated using a combination of Earth and Sun observations. The number two curves were obtained with the same number of observations but using only Earth observations. The data demonstrates the fact that the Earth observations are more important at this time. It also shows that the change in observation body did not influence the error in estimate of B•T. This would imply that this error was very likely dependent on the coordinate which cannot be determined with the Earth and Sun observations early in the flight.

In order to obtain a position estimate along the direction normal to A - A, a body must be viewed which is near the A - A direction. The region of interest is shown in Figure 2B by the cross-hatched sections. There are two alternate ways of obtaining the desired positional information as shown in the figure. Twelve hours out on the trajectory the Moon passes through the region of interest. During this time, it would be possible to obtain very fine measurements of the coordinate normal to A - A. The accuracy of measurement using the Moon at this time is shown in Figure 2A to be 8 km.

Navigation data which were generated using the Moon in conjunction with the Earth are shown in Figure 9. The significance of replacing the sun measurements with moon observations is apparent from the reduction in the error in estimate of B·T at about 5 hours along the trajectory. At this time the Moon began yielding information on the previously unknown position coordinate.

An alternate method of gaining information on the undetermined coordinate without using the Moon is to use Sun observations starting at 40 days. At this time, the Sun enters the region of interest and takes 40 days to cross it. The tracking data shown in Figure 10 makes use of the Sun during the first hundred days in conjunction with the Earth. As can be seen in that figure at about 40 days, the Sun observations have the same influence on the error in estimate of B·T as the moon does (Figure 9). The improvement in estimate is not as great as when the Moon was used. This would be expected when comparison is made of the accuracies associated with the Moon and Sun shown in Figure 2A for the times when they were used.

During the second half of the trajectory, Mars is in a position to maintain the positional information along the A - A direction. The Earth and Sun are in a position to permit estimation of the vehicle's position normal to A - A, although the quality of the measurement is poor. Therefore, over the second half of the flight, it is possible to have near-orthogonal directional coverage of the trajectory plane with the use of Mars and either the Earth or Sun.

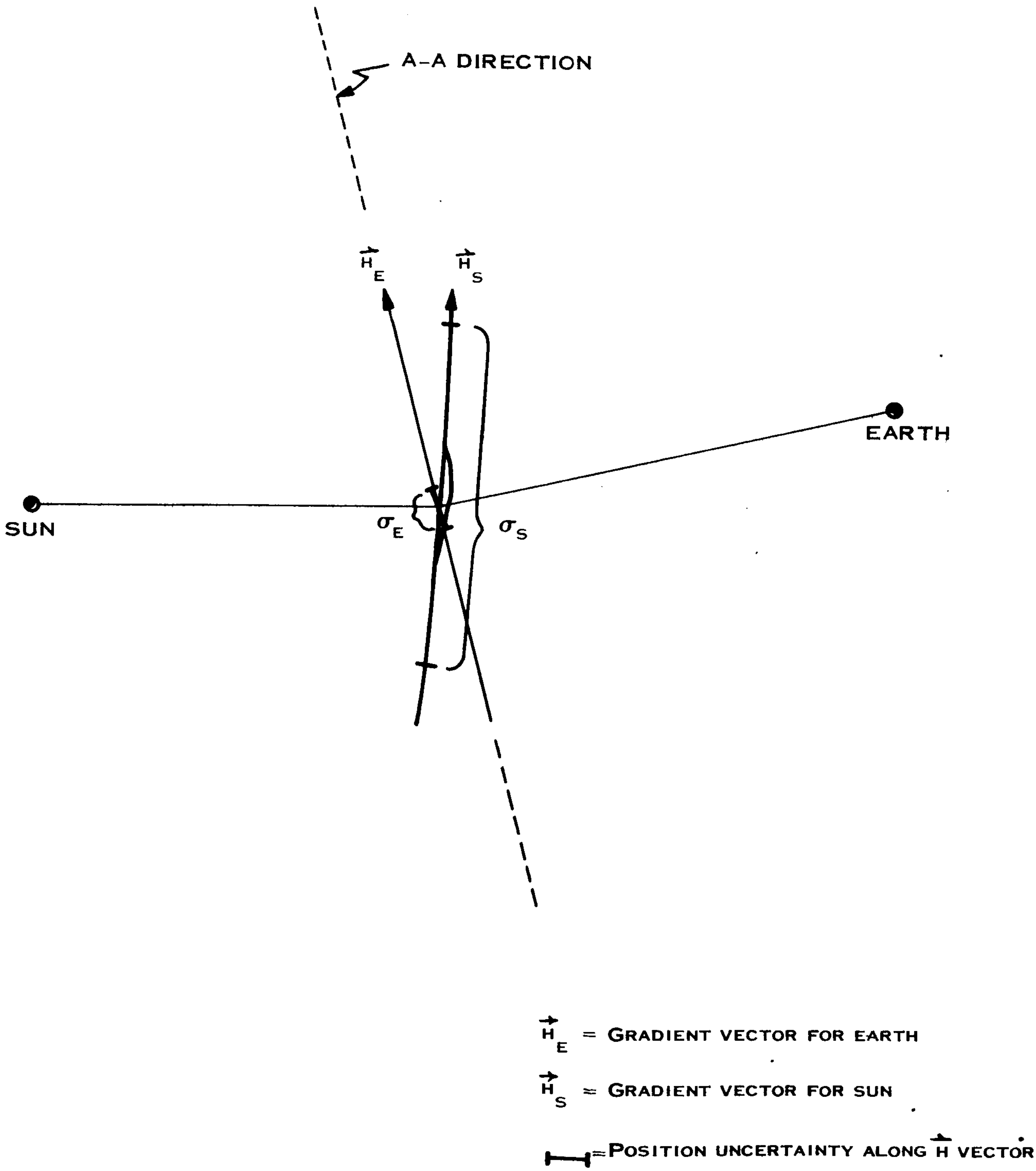


FIGURE 7. SUN-EARTH GEOMETRY EARLY IN FLIGHT ON EARTH-MARS TRAJECTORY

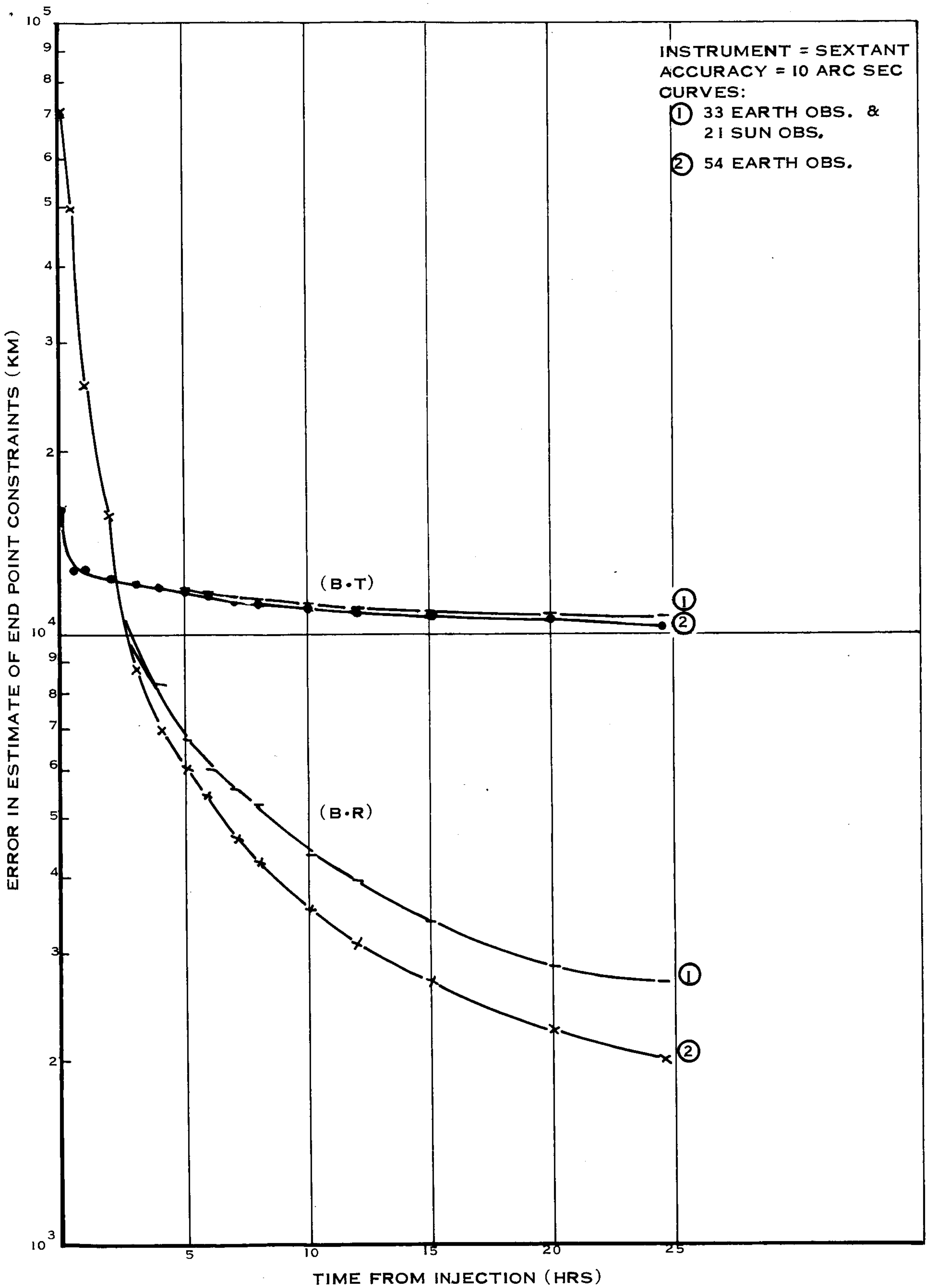


FIGURE 8. INFLUENCE OF USING SUN OBSERVATIONS EARLY ON THE EARTH-MARS TRAJECTORY

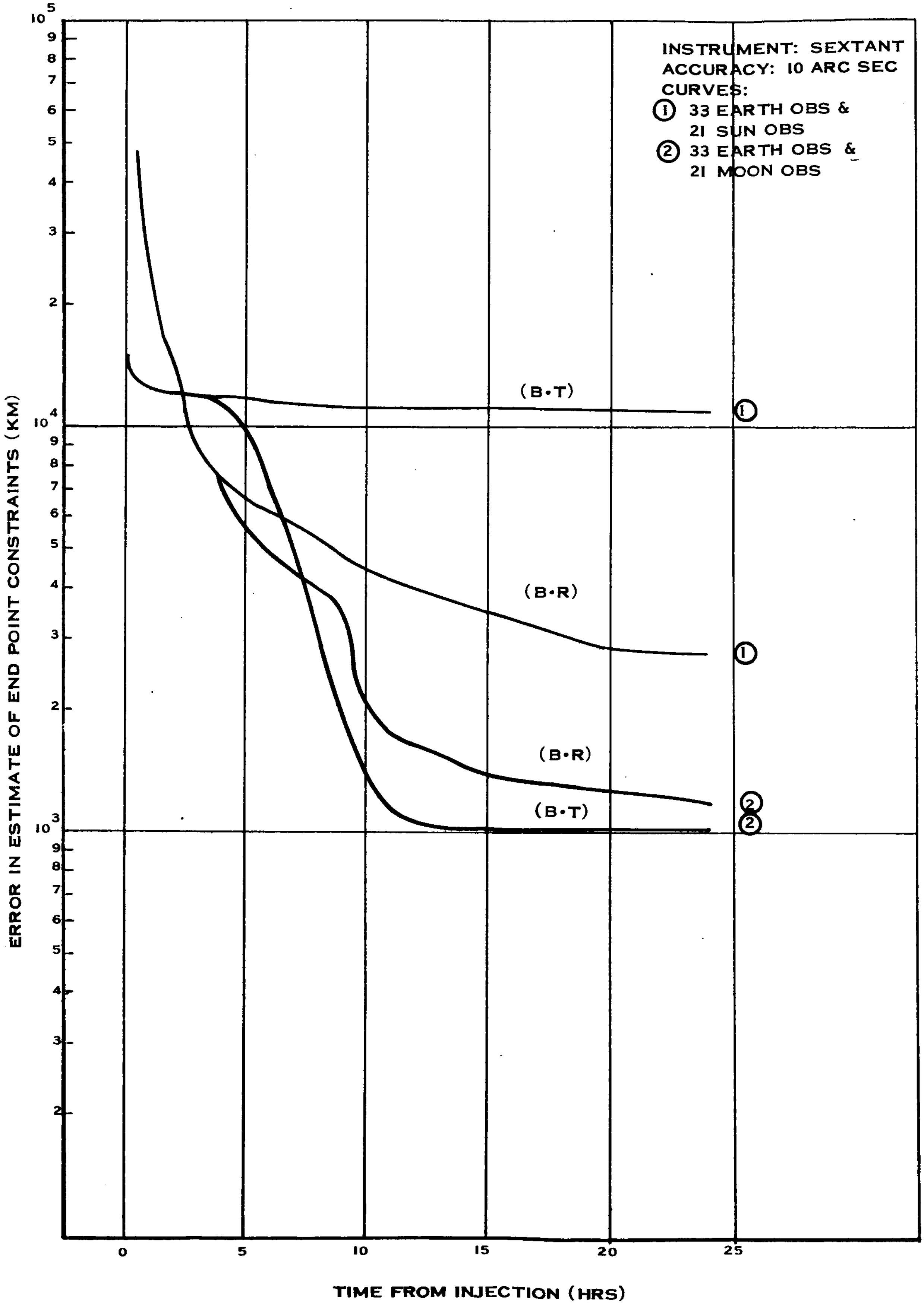


FIGURE 9. INFLUENCE OF USING MOON OBSERVATIONS ON THE EARTH-MARS TRAJECTORY

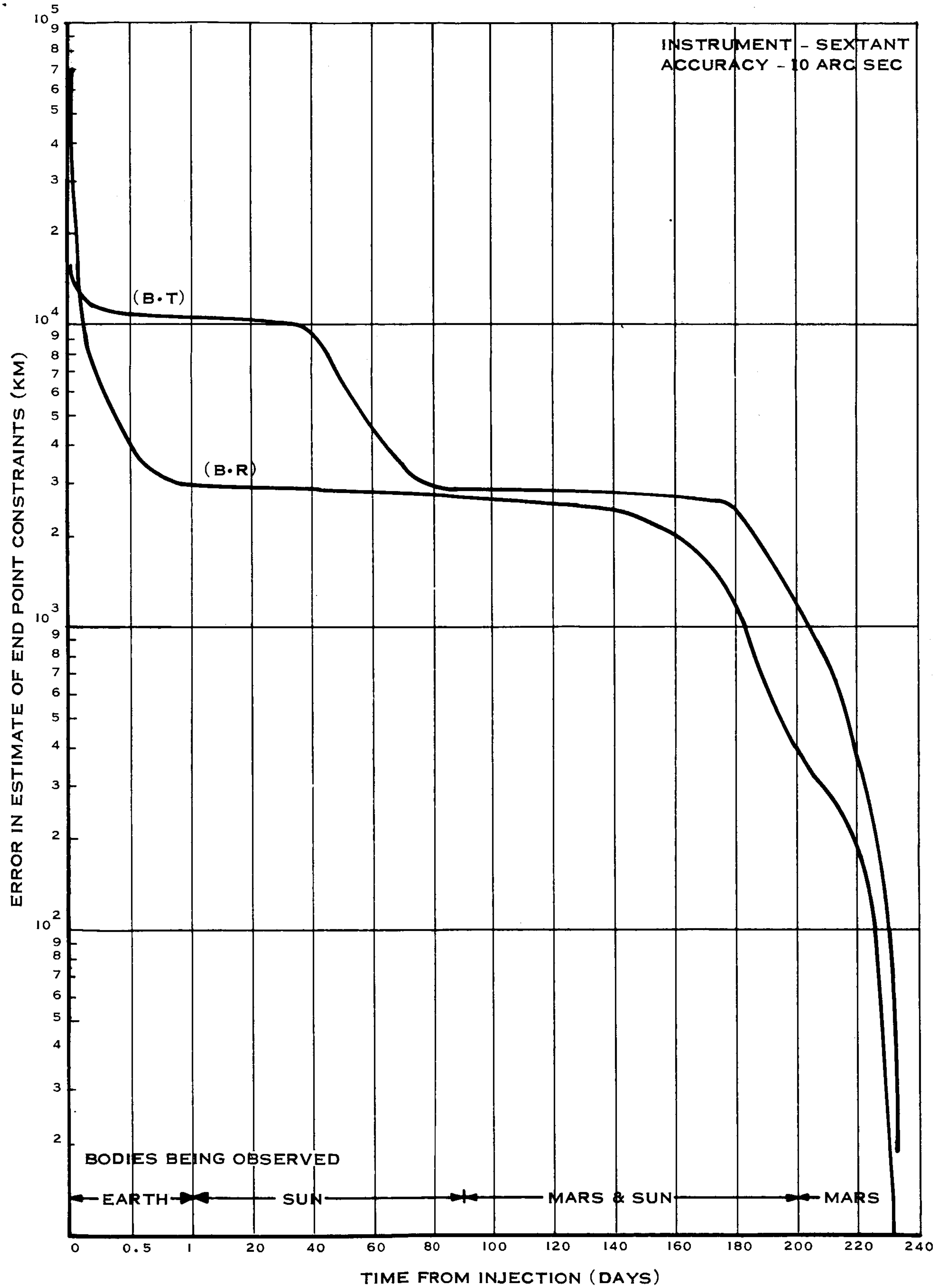


FIGURE 10. TRACKING DATA FOR EARTH-MARS TRAJECTORY

2. Mars-Earth Trajectory. The same type of auxiliary data described above is presented in Figure 5 for the Mars-Earth return trajectory. For this trajectory, the bodies of interest early in the flight, based on measurement accuracy data shown in Figure 5A, are Earth and Mars. The dominant body, Mars, exhibits the same type of directional motion as the Earth did on the out-bound mission. It changes approximately 100 degrees in the first 30 minutes, and then its direction remains extremely constant for 100 days. As described in the previous section, this body would be extremely good for determination of the spacecraft's position in the B - B directions shown in Figure 5B. The second feature of interest is selection of a body in the shaded area for determination of the position in the direction normal to B - B. This is where the return trajectory differs from the outbound. On the outbound trajectory, the primary body of interest early in flight and both secondary bodies were nearly colinear, but on the return trajectory, the primary body and two secondary bodies of interest are nearly orthogonal. The desirability of this geometry is illustrated by the tracking data shown in Figure 11. The number one curves illustrate only the use of Mars tracking. These data exhibit the same type of characteristics as the outbound trajectory data early in flight. The error in estimate remains relatively constant during the time when additional observations are being taken. This is because only one position coordinate is being estimated, and the miss estimation error remains large due to the undetermined position state. The second and third curves in Figure 11 demonstrate the value of the earth and sun being in a nearly orthogonal direction to Mars. The data for curves two and three were obtained by maintaining the same number of observations as were used for curves one, but the measurements were divided between Mars and the secondary body.

As would be expected from the measurement accuracy data shown in Figure 5A, the use of the Earth is of more value than the use of the Sun. The measurement error for an Earth observation is approximately one half that of a sun observation.

The data shown in Figure 5B also indicates a problem in the use of the earth early in the flight. The Earth as viewed from the spacecraft is about 30 degrees away from the Sun and moves toward it. At about 30 days along the trajectory, the Earth occults the Sun. Therefore, there is a region around 30 days when it would not be practical to use the Earth for obserations.

Over the last 100 days of the trajectory, the Earth and Sun are the two bodies of interest. These two bodies have an angular separation which varies from 75 degrees at 200 days to 90 degrees at 220 days to 108 degrees at the end point. Therefore, over the major part of this section of the trajectory, measurements of the earth and sun will provide total inplane position estimates. The tracking data for the entire trajectory shown in Figure 12 illustrates the fact that, for the whole trajectory, the geometry of the planetary bodies is such as to permit the total position state to be estimated at all times. This is indicated by the continual improvement of both end point estimates as more data are processed. These tracking data have a character which is quite different from the data shown in Figure 10 for the outbound mission. There are regions in this data when little or no improvement (flat regions) is obtained with additional observations. This is due to the fact that the geometry does not allow the total position state to be estimated at all times.

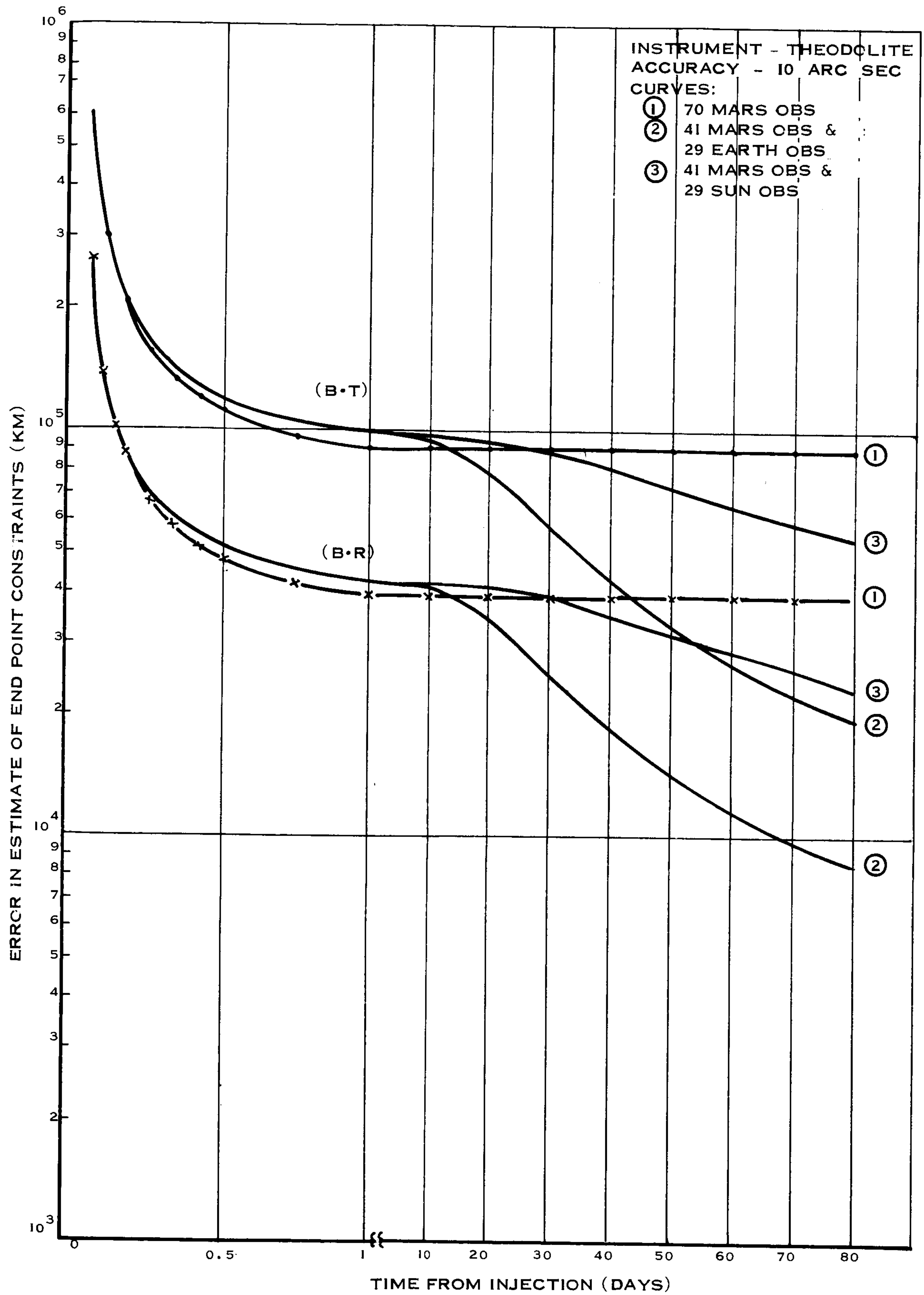


FIGURE 11. TRACKING DATA EARLY ON THE MARS-EARTH TRAJECTORY

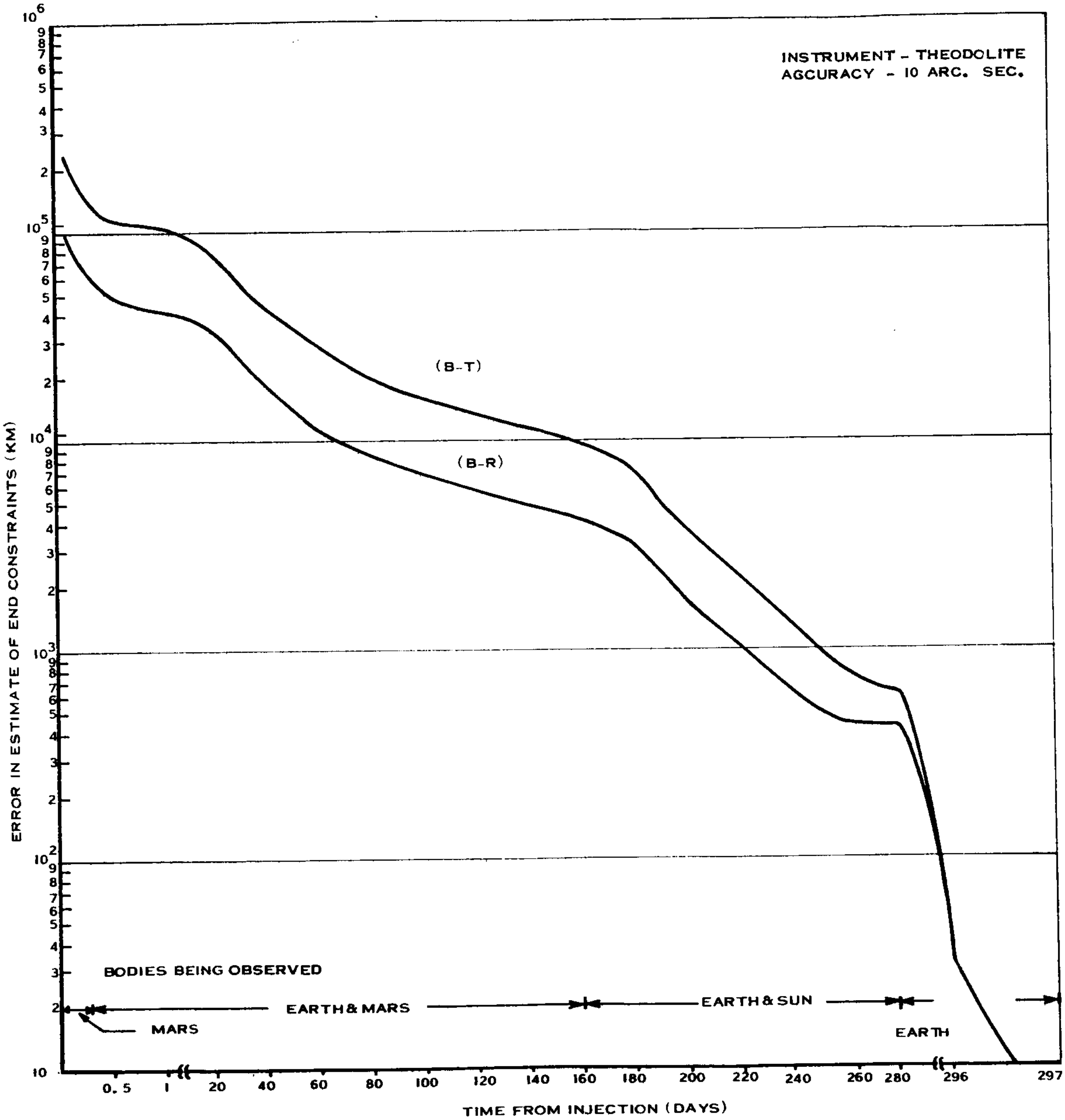


FIGURE 12. TRACKING DATA ON MARS-EARTH TRAJECTORY

3. Lunar Trajectory. The auxiliary schedule data for the lunar mission are presented in Figure 6. The measurement accuracy data shown in Figure 6A illustrates quite strongly that the only tracking bodies of interest are the earth and moon. For the launch data which was selected, the Sun is in an unfavorable position for earth observations. But, as shown in Section IV, C, changing the launch date by a few days will correct the problem.

The data in Figure 6B indicates that the directions of the Earth and Moon are 30 degrees from being colinear. With the good measurement accuracy which is associated with each body, it is very likely that the 30-degree angular separation will permit a determination of the total position. The measurement geometry is shown pictorially in Figure 13. The tracking data shown in Figure 14 tends to indicate that the total position is being estimated at all times. The error in estimate of the terminal constraints continually decreases as additional data are taken.

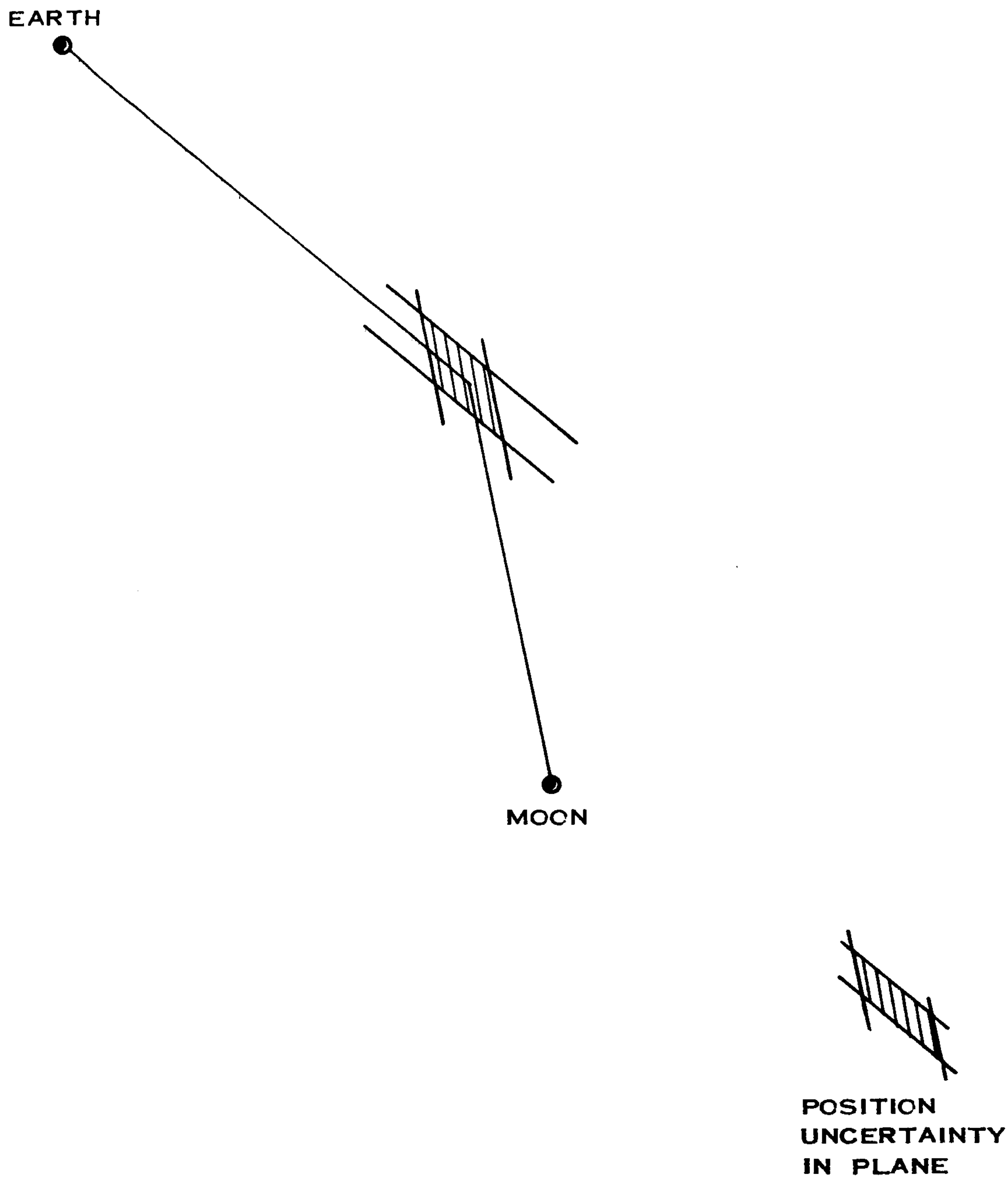


FIGURE 13. EARTH-MOON MEASUREMENT GEOMETRY

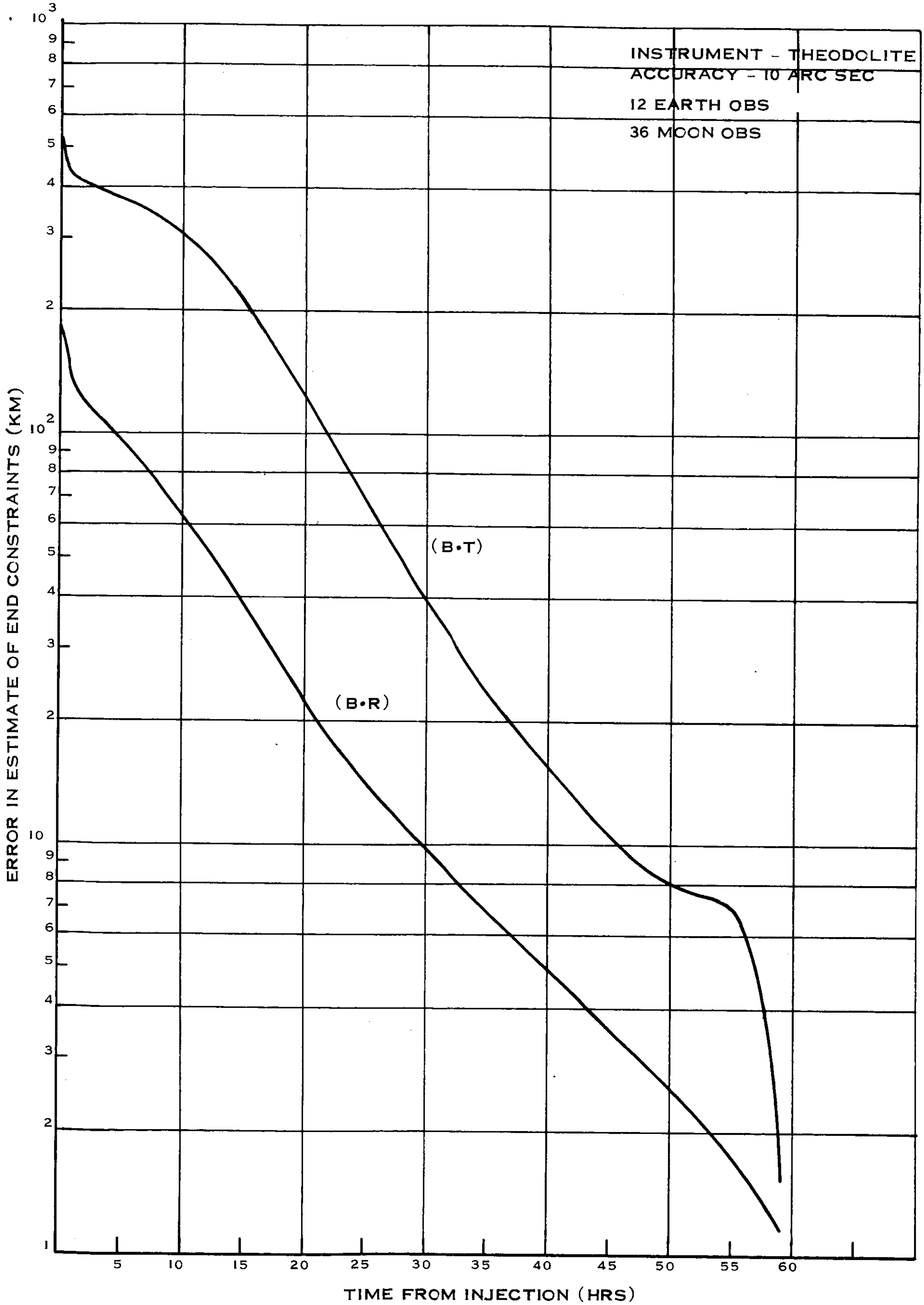


FIGURE 14. TRACKING DATA FROM A LUNAR TRAJECTORY

## SECTION IV. STAR SELECTION

### A. GENERAL

The data which are presented in this section are designed to aid in the selection of specific stars for use in making sextant observations of a planetary body. The star data presented here are to be used in conjunction with the planetary body selection data in Section III. The star data in this section indicates the availability of stars in a specific direction relative to a planetary body for use with the various bodies as a function of time.

If the line-of-sight to the planet is to be determined, two different stars must be selected for the two measurements (Figure 15).

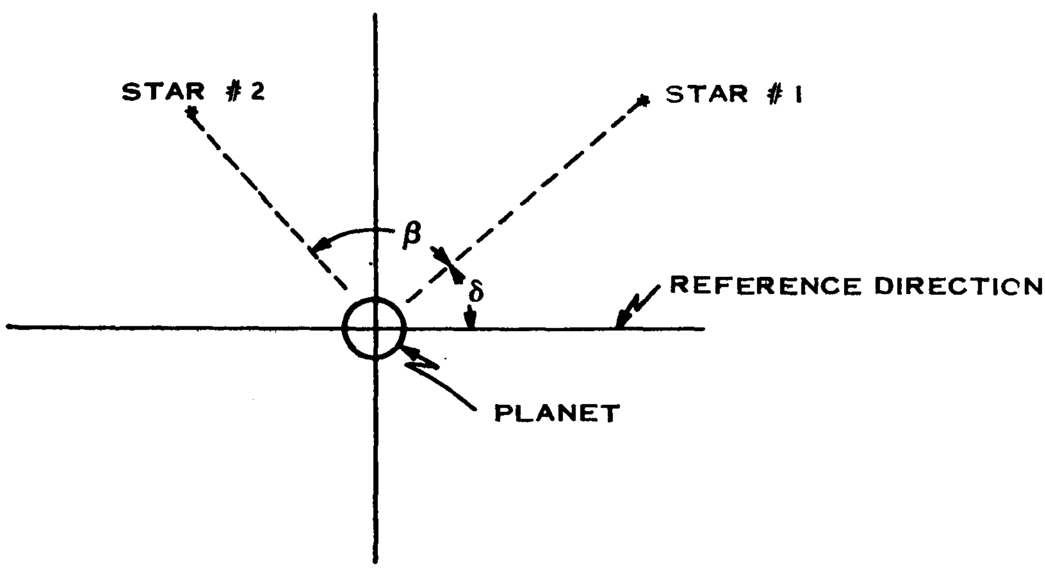


FIGURE 15. STAR SELECTIONS FOR SEXTANT MEASUREMENTS

The selection of the stars such that the angle $\beta$ is 90 degrees then yields a measurement of the LOS direction with an accuracy which is equivalent to a theodolite measurement of the LOS direction. Figure 16 demonstrates this equivalence for an Earth-to-Mars trajectory. Shown on the figure is the RMS error in estimate of position miss (B·T and B·R) at Mars encounter as a function of the time from earth injection. These data were obtained by means of the error propagation program described in Section III, D. As is seen from the figure, the two tracking schemes are effectively identical. Both provide an error in the estimate of the miss of about 10 km at Mars encounter (235 days of tracking).

The reference direction shown in Figure 15 is arbitrary when two sextant measurements are made at each point. One questions, if this reference were properly selected, would one of the measurements be more important than the other? To establish an importance, we recognize the fact that the principal cause of uncertainties in the estimate of the terminal miss can be attributed to the error in estimate of current velocity. Therefore, it would be reasonable to choose the reference direction of Figure 15 such that, for the two measurements under consideration:

1. Star No. 1 is in the direction of maximum rotation rate of the line-of-sight due to the vehicle's inertial velocity.*
2. Star No. 2 is in the direction of zero rotation rate of the line-of-sight due to the vehicle's inertial velocity.*

The No. 1 star-planet measurement then yields the greatest information on the vehicle's velocity if it is taken periodically over a given time period. Therefore, if for some reason the total number of measurements is restricted, then more measurements of this type should be assigned to the schedule than those using the star No. 2 planet measurement.

The direction of the maximum LOS rate due to the vehicle's motion is given by:

$$\hat{u} = \frac{r \times v}{|r \times v|} \times \frac{r}{|r|} \qquad (8)$$

and the direction of zero LOS rate due to the vehicle's motion is given by:

$$\hat{t} = \frac{r \times v}{|r \times v|} \qquad (9)$$

where

r = instantaneous inertial vector between the vehicle and the body

---

* In the above, the words, "due to the vehicle's inertial velocity" are added. This is imply the result of the fact that the observed celestial body ephemeris in the star background is accurately known and the knowledge of the celestial body's velocity provides no information to the estimate of the vehicle's position or velocity.

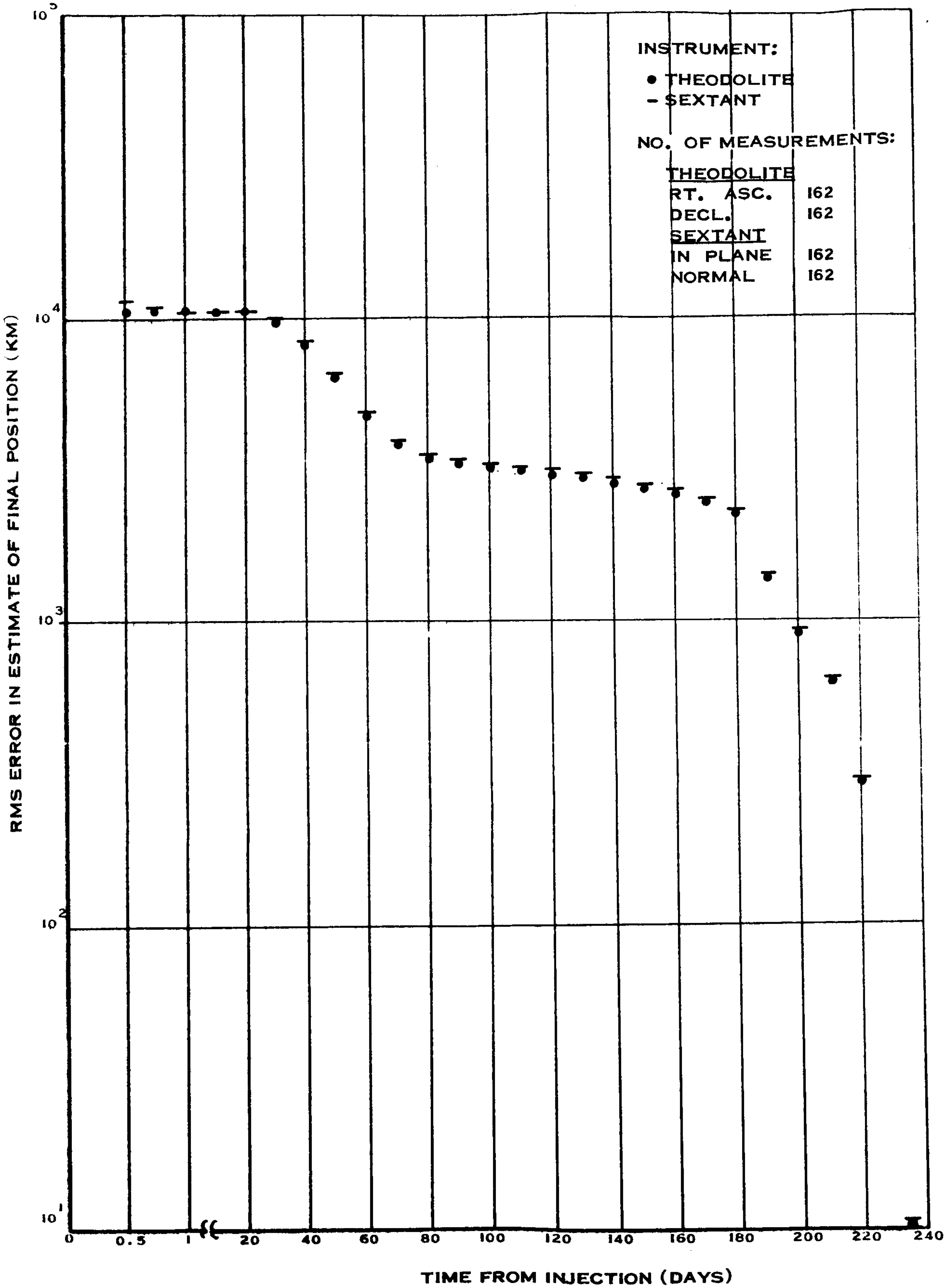


FIGURE 16. COMPARISON OF ORBIT DETERMINATION WITH A THEODOLITE AND A SEXTANT

v = the inertial velocity vector of the vehicle relative to the body of greatest attractive force, (the central body)

The velocity vector, v, is defined in this manner since the central body's inertial velocity is known and does not contribute any knowledge about the vehicle motion.

## B. EARTH-MARS TRAJECTORY

The direction of the LOS, and the $\hat{u}$ and $\hat{t}$ measurement directions for each of the planetary bodies have been generated for the Earth-Mars trajectory. The data were generated as right ascension and declination measured in vehicle-centered Earth equator of 1950 coordinates. This permits the data to be presented on star charts which are available. Figures 17A and 17B present an illustration of the information which is available from the data.

The data presented in Figure 17A is the right ascension of Earth, Mars, and Sun in Earth equator of 1950 as a function of time along the trajectory. Figure 17B is the celestial sphere as seen from the spacecraft. The dotted line is the ecliptic plane projected on the sphere. The figure also contains a few of the first, second, and third magnitude stars which are near the ecliptic plane.

Due to injection energy considerations, the interplanetary trajectory is confined to be near the ecliptic plane. The result is that all the planetary bodies will appear to be very near the ecliptic when viewed from the spacecraft. In addition, the $\hat{u}$ and $\hat{t}$ measurement directions for use with the sextant will be essentially in the ecliptic plane and normal to it respectively. As a result of this, the data shown in Figure 17 can be used for a rapid evaluation of the availability of stars as a function of time along the trajectory by projection of the RA curves into the ecliptic plane. This plane provides the required declinations for the bodies at all times. When one or more of these bodies has been selected for use with a sextant based on the data presented in Section III, the feasibility of using the body can be determined by the data shown in the figure. The availability of stars and the position of the sun can be evaluated to determine if the measurement is possible. In order to illustrate the use of Figure 17 and also indicate how vehicle constraints may be included in the selection of stars, an example will be carried through.

Assuming that data in Section III indicates that observations of the Sun and Earth are desirable at approximately 120 days, Figure 17A is entered at this time. As shown by the dotted lines, the right ascensions of these bodies are projected into the ecliptic plane shown on the celestial sphere in Figure 17B. The intersection of the dotted lines and the ecliptic plane represents the positions of the sun and earth on the celestial sphere as viewed from the spacecraft at 120 days along the trajectory. Forty by sixty degrees sectors about each of these points have been enlarged and are shown in Figure 18. It can be seen in Figure 18 that both bodies are very near the ecliptic plane, and that the $\hat{u}$ and $\hat{t}$ measurement directions are tangent (in the plane) and normal to the plane. Overlayed on each sector is a 20-degree diameter circular window. The overlay could be made

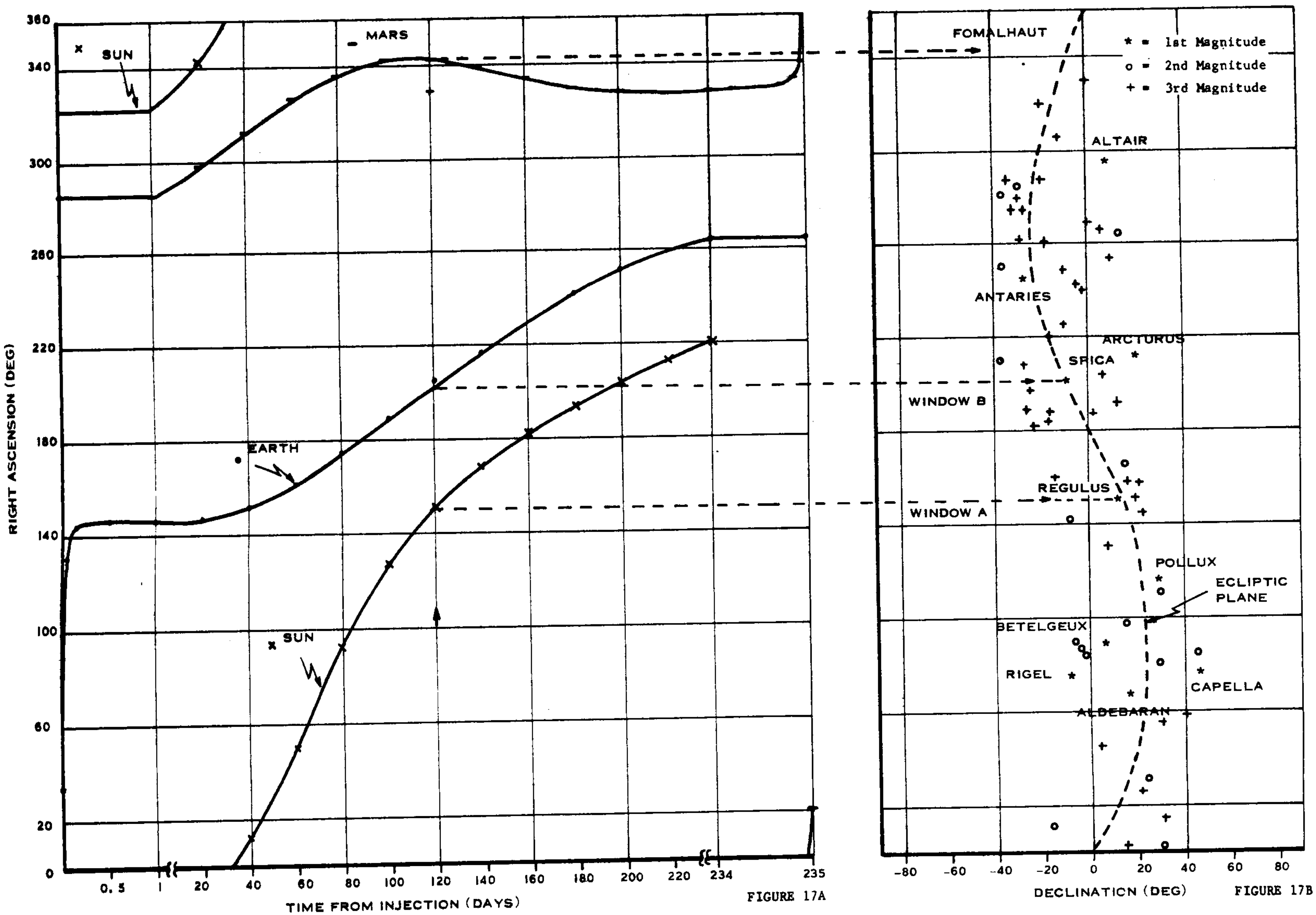


FIGURE 17. STAR SELECTION DATA

to any size and shape which corresponded to the vehicle's observation window contraints. The vehicle windows shown in the figure present the bodies of interest and the background stars available at the specified time.

The upper part of Figure 18 shows that the first magnitude star, Regulus, can be used for a measurement of the position in the $\hat{u}$ direction. The use of the star would be restricted to a slightly earlier or later time since it is directly in the sun at the time shown. The time difference which would be required would depend on the angular separation between a star and the sun required for making such a measurement when using a specific instrument. Slightly earlier in the flight (three degrees right ascension or about four days), the third magnitude star, $\gamma_{LEO}$, in the upper part of the window would be in an ideal position for a position measurement in the $\hat{t}$ direction. It is within the vehicle's window for the time shown and not too far from the reference $\hat{t}$ direction. The same type of analysis can be performed for the Earth which is shown in the lower portion of Figure 18. In this case, the star Spica could be used for a $\hat{t}$ measurement, and a few days later it would be positioned for a measurement in the $\hat{u}$ direction.

If these two bodies, Sun and Earth, were to be observed at approximately the same time, Figure 17 also indicates that the vehicle must be reoriented 52 degrees in RA and 20 degrees DEC. With a specific control system, these required excursions could be used to generate data on the time and fuel requirements for such a maneuver. The data generated in this manner would likely dictate how often one might want to switch bodies being observed.

The data in Figure 17A can also be used to evaluate the position of the sun relative to a body of interest. This would be done to ensure that the sun did not "blind" the instrument being used. For example, at the time of 120 days, the earth is 50 degrees away from the sun. The figure also indicates that this is as close as the earth gets to the sun along the whole trajectory.

## C. LUNAR TRAJECTORY

These auxiliary star selection data have been generated for a lunar trajectory and are presented in Figure 19. There are a number of features of the lunar trajectory which require that the data presentation be slightly different. First, it is shown in Section III that only bodies of interest for tracking are the earth and moon. The sun is of interest only because its position relative to these bodies could make measurements of either the earth or moon impossible. Therefore, the data shown are only concerned with these three bodies. Second, the dotted line shown in the figure is the injection trajectory plane projected on the celestrial sphere rather than the ecliptic plane. Then the RA of the earth and moon may be projected up to this line to determine the declination of the body and its position on the celestial sphere. There will be very little movement of the sun during typical lunar trajectories and it can therefore be positioned in the proper position as shown in Figure 19C. The sun will always be near the ecliptic plane, and is not projected into the trajectory plane shown by the dotted line.

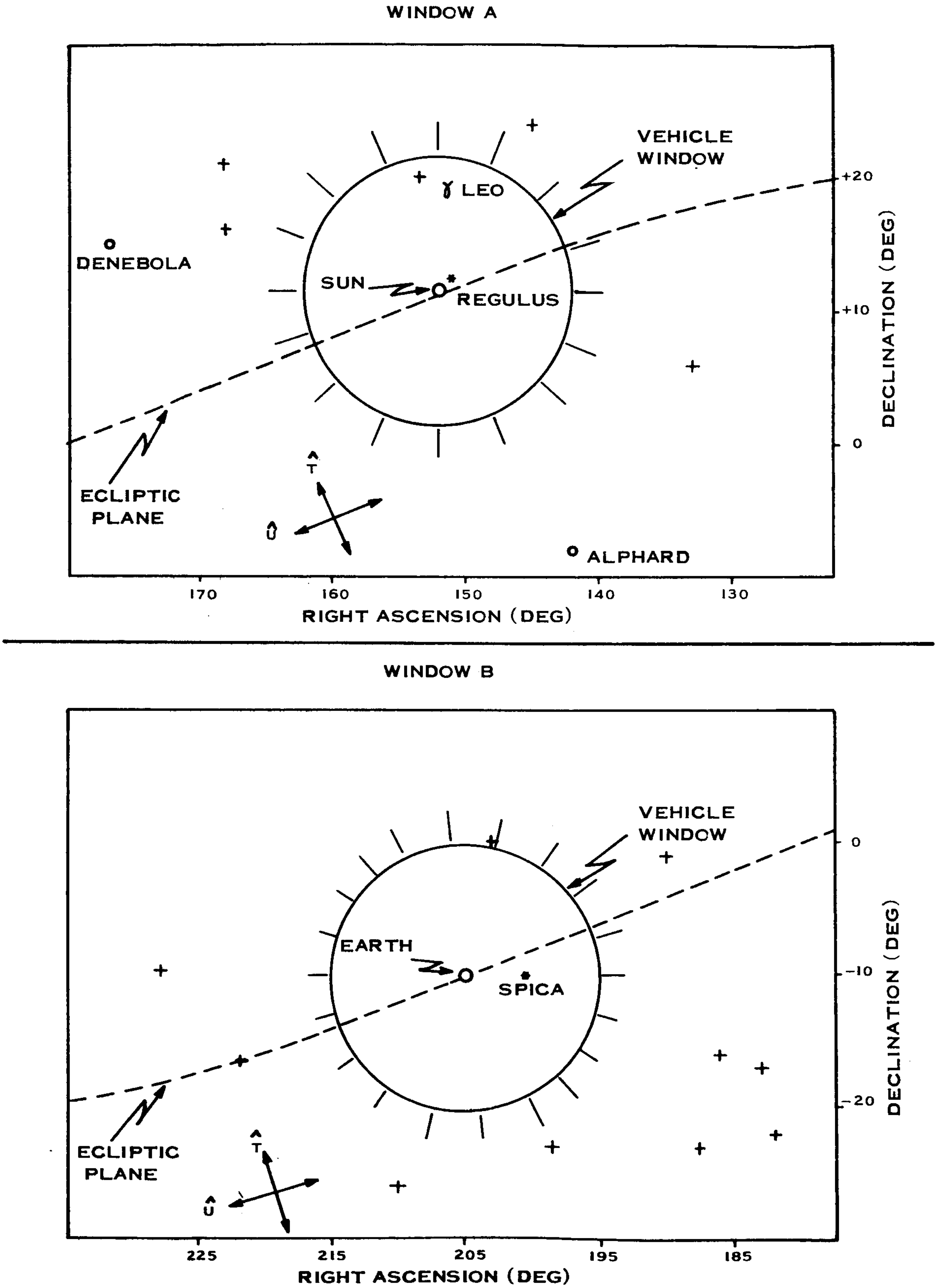


**FIGURE 18. VEHICLE OBSERVATION WINDOWS**

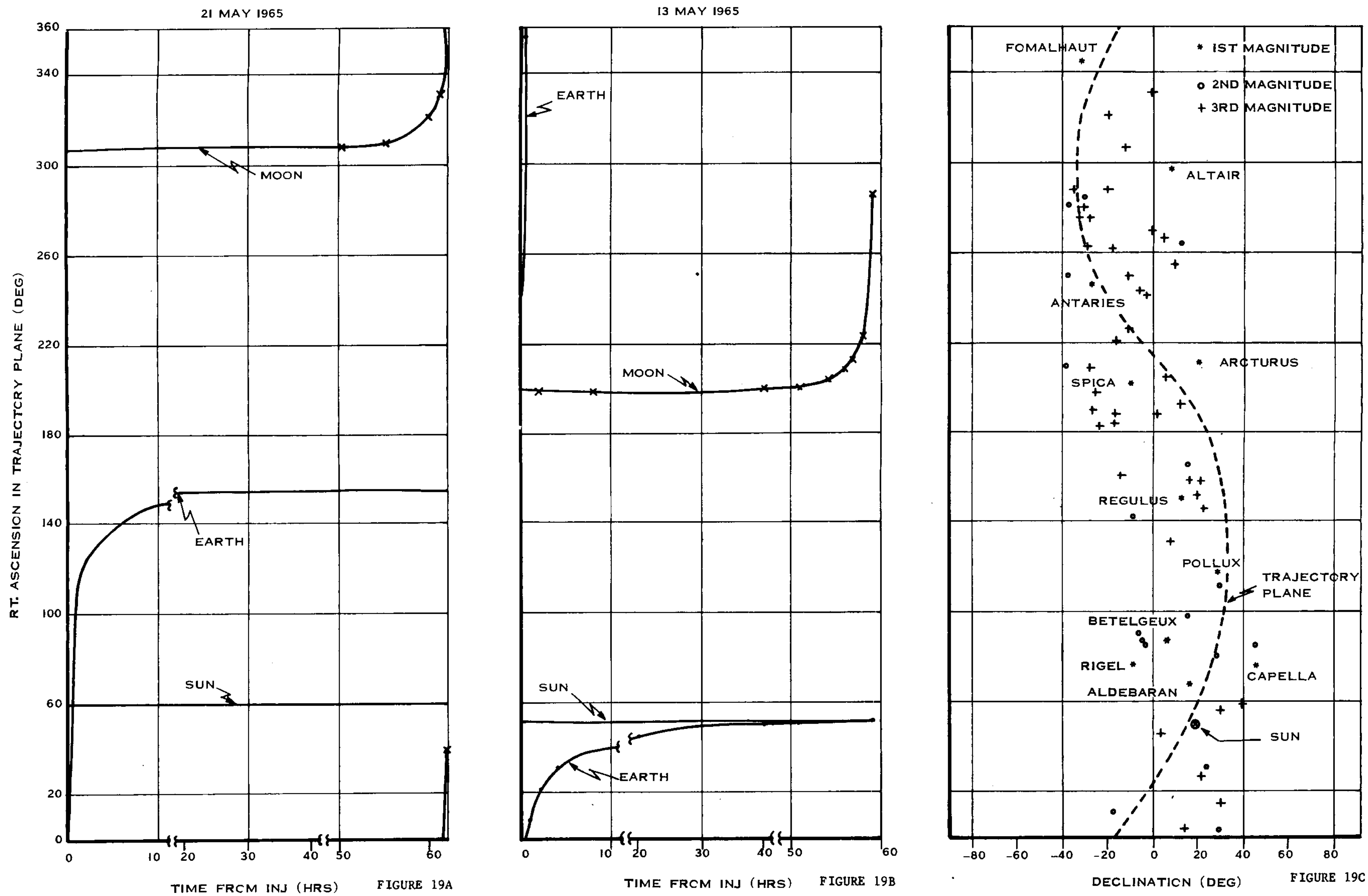


FIGURE 19. STAR SELECTION DATA FOR LUNAR TRAJECTORIES

The trajectory plane was used rather than the ecliptic because the lunar trajectory is not restricted by launch energy consideration to be near the ecliptic. The trajectory plane shown in the figure is inclined about 10 degrees to the ecliptic.

The data in Figure 19 which has been described above are then used in the same manner as described for the Earth-Mars trajectory. It is of interest to note that, with the exception of the first and last few hours of flight, the background stars for the Earth and Moon remain constant. It is, therefore, possible by selection of the appropriate time of month for a flight to obtain a desirable star background. For instance, the data shown in Figure 19B for one injection data indicates that the position of the sun would make observation of the earth impossible for most of the trajectory. The data in Figure 19A shows a more favorable position of the sun obtained by selecting a launch date eight days later. Figure 19A also indicates that the background stars for the Earth and Moon have also been changed. This shows the flexibility available in obtaining desirable tracking situations by changing the launch date for a lunar mission.

# APPENDIX A. TRAJECTORY DESCRIPTIONS

## A. GENERAL

This appendix contains a description of the three nominal trajectories which have been used to describe and evaluate the schedule data which are presented. They consist of two interplanetary trajectories (round trip to Mars) and one lunar trajectory.

## B. EARTH-MARS TRAJECTORY

The description of the trajectory is presented below with an ecliptic projection of the trajectory shown in Figure 20. The trajectory has a park time of 1736.5 seconds.

| Injection Conditions | Earth-Centered, Earth Equator 1950 |
|---|---|
| Launch Date | 10 February 1975 |
| Fractional Date | 2 Hrs., 1 Min., 25.147 Sec. |
| Range | 6563.4642 Km. |
| Right Ascension | -147.01278 Deg. |
| Declination | -19.360749 Deg. |
| Velocity | 16.058885 Km/Sec |
| Azimuth | 110.97047 Deg. |
| Path Angle | $0.38146973 \cdot 10^{-5}$ Deg. |
| Flight Time | 235 Days |

The radius of closest approach at Mars is 3860 Km.

## C. MARS-EARTH TRAJECTORY

This trajectory is the continuation of the Earth-Mars trajectory back to earth. It was assumed that there was a 40-day stay in the Martian orbit prior to return. The trajectory is shown in Figure 21 projected into the ecliptic plane.

| Injection Conditions | Mars-Centered, Earth Equator 1950 |
|---|---|
| Launch Date | 12 November 1975 |
| Fractional Date | 10 Hrs., 47 Min., 26.241 Sec. |
| Range | 3951.7483 Km |
| Right Ascension | -151.02687 Deg. |
| Declination | -9.7216896 Deg. |
| Velocity | 6.6190158 Km/Sec |

| | |
|---|---|
| Azimuth | 119.26048 Deg. |
| Path Angle | 0.59214306 Deg. |
| Flight Time | 297 Days |

The radius of closest approach at the Earth is 6442 Km.

## D. LUNAR TRAJECTORY

The lunar trajectory was selected for 1965. The trajectory is shown in Figure 22 projected on the injection trajectory plane. The trajectory has a park time of 4124.7 seconds.

| Injection Conditions | Earth-Centered, Earth Equator 1950 |
|---|---|
| Launch Date | 13 May 1965 |
| Fractional Date | 58 Min., 10.402 Sec. |
| Range | 6562.1644 Km. |
| Right Ascension | 63.238201 |
| Declination | 22.525811 |
| Velocity | 10.985436 Km/Sec |
| Azimuth | 64.422800 Deg. |
| Path Angle | $0.9073486 \cdot 10^{-5}$ Deg |
| Flight Time | 60 Hrs. |

The radius of closest approach at the Moon is 2260 Km.

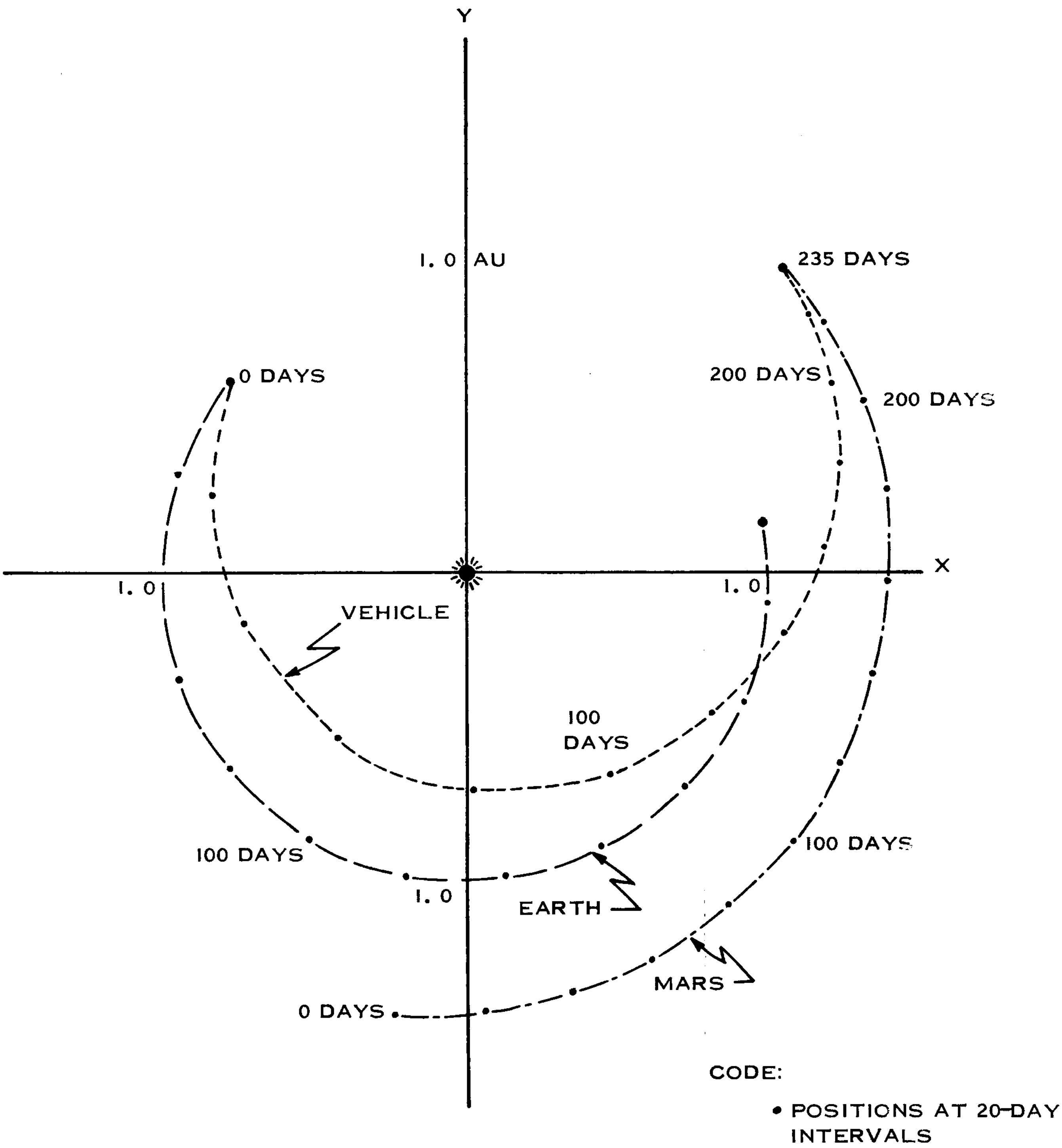


FIGURE 20. ECLIPTIC PROJECTION OF THE EARTH-MARS TRAJECTORY

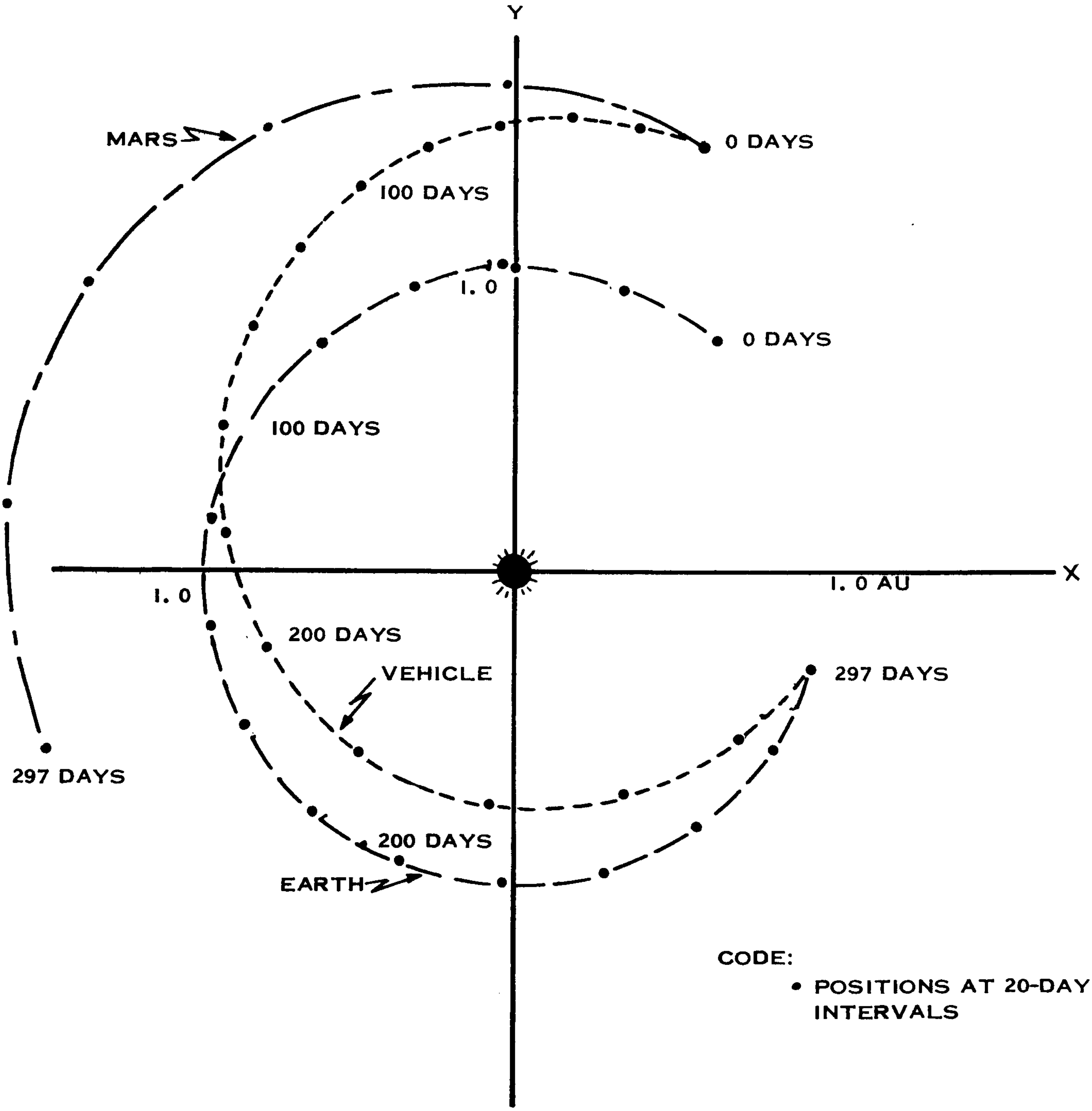


FIGURE 21. ECLIPTIC PROJECTION OF THE MARS-EARTH TRAJECTORY

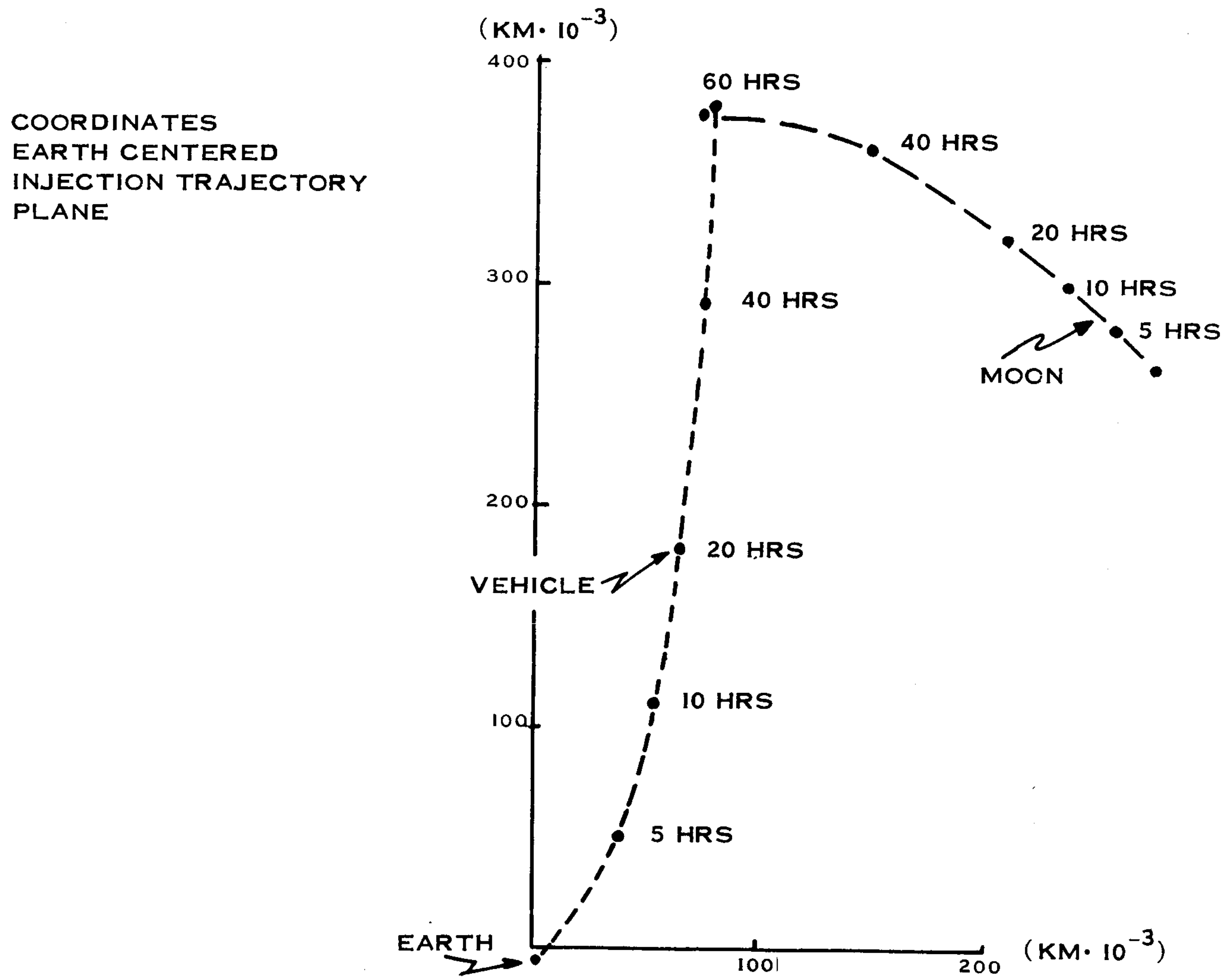


FIGURE 22. LUNAR TRAJECTORY PROJECTED ON THE INJECTION TRAJECTORY PLANE

## APPENDIX B. GRADIENT OF MEASUREMENT

### A. GENERAL

Assuming that an estimate of the trajectory of interest is available, one may use perturbation techniques in utilizing the measurements to improve the estimate. The deviation in a measurement quantity, $\delta q$, from the nominal value may be written as follows:

$$\delta q = \vec{h} \cdot x \tag{10}$$

where

$\delta q$ = deviation of measurement from nominal

$\vec{h}$ = row vector which is the gradient of the measurement with respect to the position

$x$ = position deviation state

As can be seen in Equation (10), the quantity which characterizes an individual measurement is the measurement gradient vector, $\vec{h}$.

In this appendix, a derivation of the gradient for the sextant measurement is presented. The geometrical significance of the $\vec{h}$ vectors associated with a set of measurements is explained and used in Section III.

### B. SEXTANT OBSERVATION

The gradient of the sextant measurement may be obtained as follows. The interest in the use of the sextant has been restricted to star-planet angle measurements for this derivation. The geometry of the measurement is shown in Figure 23. The quantity of interest is $\nabla_x \alpha$.

Where $\nabla_x$ is the gradient with respect to the vehicle's position state, $\vec{x}$. The subscript x will be omitted in the following derivation.

The angle, $\alpha$, which is measured with the sextant may be represented as*

$$\cos \alpha = \hat{S}_1 \cdot \hat{P}_1 = \hat{S}_1^{\,T} \hat{P}_1 \tag{11}$$

* Superscript T means transpose; I = unit diagonal matrix

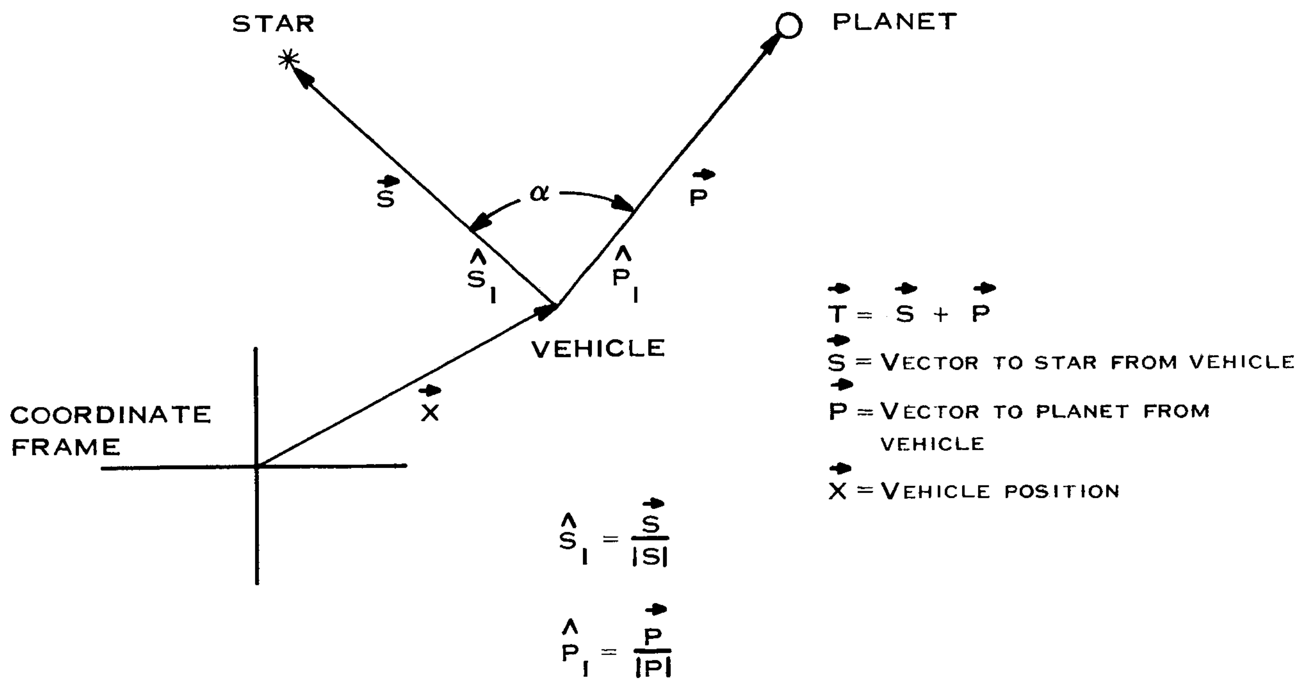


FIGURE 23. GEOMETRY OF THE SEXTANT MEASUREMENT

Taking the gradient of Equation (11) yields

$$-\sin\alpha\nabla\alpha = \hat{S}_1^T\nabla\hat{P}_1 + \hat{P}_1^T\nabla\hat{S}_1 \tag{12}$$

or

$$\nabla\alpha = -\frac{1}{\sin\alpha}\left(\hat{S}_1^T\nabla\hat{P}_1 + \hat{P}_1^T\nabla\hat{S}_1\right) \tag{12A}$$

The unit vector, $S_1$, pointing to a star is not a function of vehicle position; therefore

$$\nabla\hat{S}_1 = 0$$

and Equation (12A) becomes

$$\nabla\alpha = -\frac{1}{\sin\alpha}\left(\hat{S}_1^T\nabla\hat{P}_1\right) \tag{13}$$

The gradient of $P_1$ may be rewritten as

$$\nabla \hat{P}_1 = \nabla\left(\frac{\vec{P}}{|P|}\right) = \frac{1}{|P|}\nabla \vec{P} + \vec{P}\nabla\frac{1}{|P|}$$

$$= \frac{1}{|P|}\nabla \vec{P} - \vec{P}\,\vec{P}^T \frac{\nabla P}{|P|^3} \tag{14}$$

$$= \frac{1}{|P|}\left(I - \frac{\vec{P}\,\vec{P}^T}{|P|^2}\right)\nabla \vec{P}$$

Substitute of Equation (14) into Equation (13) yields:

$$\nabla \alpha = - \frac{\hat{S}_1^{\,T}}{|P| \sin \alpha}\left(I - \hat{P}_1\,\hat{P}_1^{\,T}\right)\nabla \vec{P} \tag{15}$$

For the direction of the vectors $\vec{x}$ and $\vec{P}$ shown in Figure 24, the gradient of $\vec{P}$ with respect to $\vec{x}$ is

$$\nabla_x \vec{P} = - I$$

therfore Equation (15) becomes:

$$\nabla \alpha = \frac{\hat{S}_1^{\,T}}{|P| \sin \alpha}\left(I - \hat{P}_1\,\hat{P}_1^{\,T}\right) = \frac{1}{|P|}\left\{\frac{\hat{P}_1 \times \hat{S}_1}{|\hat{P}_1 \times \hat{S}_1|} \times \hat{P}_1\right\} \tag{16}$$

The two parts of Equation (16) which are of interest are the matrix, $(I - \hat{P}_1\hat{P}_1^{\,T})$ and the vector $\hat{S}_1^{\,T}$

The matrix, $(I - \hat{P}_1\hat{P}_1^{\,T})$, will project any vector into a plane normal to the vector $\hat{P}_1$. The gradient of the measurement will therefore lie in a plane normal to the direction of the line-of-sight to the planet being used. The unit vector, $\hat{S}_1$, is therefore projected into a plane normal to the line-of-sight. This projected vector establishes the direction of the gradient in the plane normal to the line-of-sight. Therefore, the direction of the measurement gradient is described by the intersection of two planes. One plane is normal to the direction of line-of-sight and the second plane is the one which contains the vehicle, planet and star.

Contract NAS8-11198 - Philco Corporation, WDL Division

DISTRIBUTION LIST

MSFC

| | |
|---|---|
| R-ASTR-DIR | Dr. Haeussermann |
| R-ASTR-A | Mr. Digesu<br>Mr. Pavlick<br>Mr. Daniel<br>Mr. Hamilton<br>Mr. Harden (3)<br>Mr. MacCrone |
| R-ASTR-BC | Mr. Thornton |
| R-ASTR-N | Mr. Seltzer<br>Mr. Drawe |
| R-ASTR-G | Mr. Thomason<br>Mrs. Neighbors |
| R-ASTR-I | Mr. Mixon |
| R-ASTR-R | Mr. Taylor |
| R-ASTR-CF | |
| R-AS | Mr. deFries<br>Mr. Ruppe |
| R-AERO-F | Mr. Hill |
| R-AERO-D | Mr. Hart |
| MS-IP | |
| MS-IL (8) | |

| | |
|---|---|
| Langley Research Center<br>Langley Field, Virginia | Mr. John Dodgen<br>Mr. W. Crosswell |
| Manned Spacecraft Center<br>Houston, Texas | Mr. R. Chilton<br>Mr. R. Sawyer |
| Ames Research Center<br>Moffett Field, California | Mr. J. White<br>Dr. H. Hornby |
| Wright-Patterson AFB, Ohio<br>Navigation and Guidance Laboratory<br>Aeronautical Systems Division | Mr. R. J. Doran |
| Wright-Patterson AFB, Ohio<br>AF Avionics Laboratory<br>Research and Technology Division | Mr. A. Goldman |
| Bureau of Naval Weapons<br>Code RT-2<br>Washington, D. C. | Mr. H. Antzes |
| Institute of Naval Studies<br>185 Alewife<br>Brook Parkway<br>Cambridge, Massachusetts | Dr. C. Mundo |
| Cornell Aeronautical Laboratories<br>4355 Genesee Street<br>Buffalo 21, New York | Mr. R. Taylor |
| Hughes Aircraft Company<br>Culver City, California | Dr. L. Bailin |
| Clemson College<br>Clemson, South Carolina | Dr. C. Aucoin |
| University of Tennessee<br>Knoxville, Tennessee | Dr. J. Hung |
| Space Technology Laboratory<br>No. 1 Space Park<br>Los Angeles, California | Mr. J. Holland |

| | |
|---|---|
| Philco Corporation<br>Western Development Laboratory<br>3875 Fabian Way<br>Palo Alto, California | Dr. S. Schmidt |
| Sylvania Company<br>Huntsville, Alabama | Mr. J. Weaver |
| Ryan Aeronautical Company<br>Holiday Office Center<br>Huntsville, Alabama | Mr. Sucop |
| Bendix Corporation<br>Holiday Office Center<br>Huntsville, Alabama | Mr. W. Uline |
| Emerson Electric Company<br>8100 Florissant Avenue<br>St. Louis, Missouri | Mr. Ralph Mitchell |
| Sperry Gyroscope Company<br>3313 Memorial Parkway<br>Sahara Office Park<br>Suite 127<br>Huntsville, Alabama | Mr. Howard Thames |
| Electronics Research Center<br>575 Technology Square<br>Cambridge, Massachusetts | Mr. Ernest Steele |
| Scientific and Technical Inf. Facil. (2)<br>Attn: NASA Rep. (S-AK RKT)<br>P.O. Box 33<br>College Park, Maryland 20740 | |